Critical role of PA28γ in hepatitis C virus-associated steatogenesis and hepatocarcinogenesis

Kohji Moriishi*, Rika Mochizuki*, Kyoji Moriya†, Hironobu Miyamoto*, Yoshio Mori*, Takayuki Abe*, Shigeo Murata‡, Keiji Tanaka‡, Tatsuo Miyamura§, Tetsuro Suzuki§, Kazuhiko Koike†, and Yoshiharu Matsuura*¶

*Department of Molecular Virology, Research Institute for Microbial Diseases, Osaka University, Osaka 565-0871, Japan; †Department of Internal Medicine, Graduate School of Medicine, University of Tokyo, Tokyo 113-8655, Japan; ‡Department of Molecular Oncology, Tokyo Metropolitan Institute of Medical Science, Tokyo 113-8613, Japan; and §Department of Virology II, National Institute of Infectious Diseases, Tokyo 162-8640, Japan

Edited by Peter Palese, Mount Sinai School of Medicine, New York, NY, and approved December 1, 2006 (received for review August 23, 2006)

Hepatitis C virus (HCV) is a major cause of chronic liver disease that frequently leads to steatosis, cirrhosis, and eventually hepatocellular carcinoma (HCC). HCV core protein is not only a component of viral particles but also a multifunctional protein because liver steatosis and HCC are developed in HCV core gene-transgenic (CoreTg) mice. Proteasome activator PA28γ/REGγ regulates host and viral proteins such as nuclear hormone receptors and HCV core protein. Here we show that a knockout of the PA28γ gene induces the accumulation of HCV core protein in the nucleus of hepatocytes of CoreTg mice and disrupts development of both hepatic steatosis and HCC. Furthermore, the genes related to fatty acid biosynthesis and *srebp-1c* promoter activity were up-regulated by HCV core protein in the cell line and the mouse liver in a PA28γ-dependent manner. Heterodimer composed of liver X receptor α (LXRα) and retinoid X receptor α (RXRα) is known to up-regulate *srebp-1c* promoter activity. Our data also show that HCV core protein enhances the binding of LXRα/RXRα to LXR-response element in the presence but not the absence of PA28γ. These findings suggest that PA28γ plays a crucial role in the development of liver pathology induced by HCV infection.

fatty acid | proteasome | sterol regulatory element-binding protein (SREBP) | RXRα | LXRα

Hepatitis C virus (HCV) belongs to the Flaviviridae family, and it possesses a positive, single-stranded RNA genome that encodes a single polyprotein composed of ≈3,000 aa. The HCV polyprotein is processed by host and viral proteases, resulting in 10 viral proteins. Viral structural proteins, including the capsid (core) protein and two envelope proteins, are located in the N-terminal one-third of the polyprotein, followed by nonstructural proteins.

HCV infects >170 million individuals worldwide, and then it causes liver disease, including hepatic steatosis, cirrhosis, and eventually hepatocellular carcinoma (HCC) (1). The prevalence of fatty infiltration in the livers of chronic hepatitis C patients has been reported to average ≈50% (2, 3), which is higher than the percentage in patients infected with hepatitis B virus and other liver diseases. However, the precise functions of HCV proteins in the development of fatty liver remain unknown because of the lack of a system sufficient to investigate the pathogenesis of HCV. HCV core protein expression has been shown to induce lipid droplets in cell lines and hepatic steatosis and HCC in transgenic mice (4–6). These reports suggest that HCV core protein plays an important role in the development of various types of liver failure, including steatosis and HCC.

Recent reports suggest that lipid biosynthesis affects HCV replication (7–9). Involvement of a geranylgeranylated host protein, FBL2, in HCV replication through the interaction with NS5A suggests that the cholesterol biosynthesis pathway is also important for HCV replication (9). Increases in saturated and monounsaturated fatty acids enhance HCV RNA replication, whereas increases in polyunsaturated fatty acids suppress it (7). Lipid homeostasis is regulated by a family of steroid regulatory element-binding proteins (SREBPs), which activate the expression of >30 genes involved in the synthesis and uptake of cholesterol, fatty acids, triglycerides, and phospholipids. Biosynthesis of cholesterol is regulated by SREBP-2, whereas that of fatty acids, triglycerides, and phospholipids is regulated by SREBP-1c (10–14). In chimpanzees, host genes involved in SREBP signaling are induced during the early stages of HCV infection (8). SREBP-1c regulates the transcription of acetyl-CoA carboxylase, fatty acid synthase, and stearoyl-CoA desaturase, leading to the production of saturated and monounsaturated fatty acids and triglycerides (15). SREBP-1c is transcriptionally regulated by liver X receptor (LXR) α and retinoid X receptor (RXR) α, which belong to a family of nuclear hormone receptors (15, 16). Accumulation of cellular fatty acids by HCV core protein is expected to be modulated by the SREBP-1c pathway because RXRα is activated by HCV core protein (17). However, it remains unknown whether HCV core protein regulates the *srebp-1c* promoter.

We previously reported (18) that HCV core protein specifically binds to the proteasome activator PA28γ/REGγ in the nucleus and is degraded through a PA28γ-dependent pathway. PA28γ is well conserved from invertebrates to vertebrates, and amino acid sequences of human and murine PA28γs are identical (19). The homologous proteins, PA28α and PA28β, form a heteroheptamer in the cytoplasm, and they activate chymotrypsin-like peptidase activity of the 20S proteasome, whereas PA28γ forms a homoheptamer in the nucleus, and it enhances trypsin-like peptidase activity of 20S proteasome (20). Recently, Li and colleagues (21) reported that PA28γ binds to steroid receptor coactivator-3 (SRC-3) and enhances the degradation of SRC-3 in a ubiquitin- and ATP-independent manner. However, the precise physiological functions of PA28γ are largely unknown *in vivo*. In this work, we examine whether PA28γ is required for liver pathology induced by HCV core protein *in vivo*.

Results

PA28γ-Knockout HCV Core Gene Transgenic Mice. To determine the role of PA28γ in HCV core-induced steatosis and the development of HCC *in vivo*, we prepared PA28γ-knockout core gene transgenic mice. The PA28γ-deficient, PA28γ$^{-/-}$ mice were born without

Author contributions: K. Moriishi, K.T., T.M., T.S., K.K., and Y. Matsuura designed research; K. Moriishi, R.M., K. Moriya, H.M., Y. Mori, and T.A. performed research; S.M. contributed new reagents/analytic tools; Y. Matsuura analyzed data; and K. Moriishi, K.K., and Y. Matsuura wrote the paper.

The authors declare no conflict of interest.

This article is a PNAS direct submission.

Freely available online through the PNAS open access option.

Abbreviations: CoreTg, HCV core gene-transgenic; HCC, hepatocellular carcinoma; HCV, hepatitis C virus; LXR, liver X receptor; LXRE, liver X receptor-response element; MEF, mouse embryonic fibroblast; ROS, reactive oxygen species; RXR, retinoid X receptor; SRC-3, steroid receptor coactivator-3; SREBP, steroid regulatory element-binding protein.

¶To whom correspondence should be addressed. E-mail: matsuura@biken.osaka-u.ac.jp.

This article contains supporting information online at www.pnas.org/cgi/content/full/0607312104/DC1.

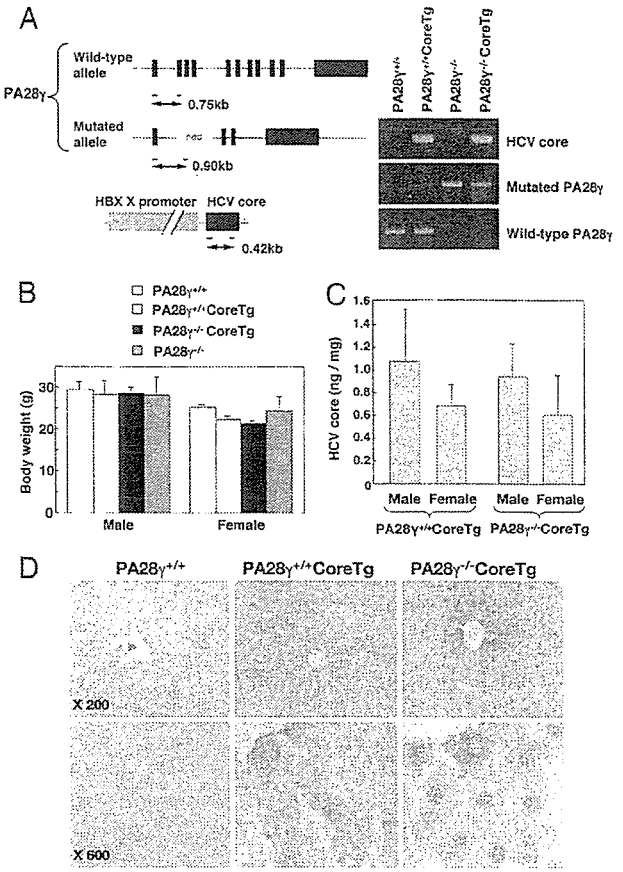

Fig. 1. Preparation and characterization of PA28γ-knockout HCV core-transgenic mice. (*A*) The structures of the wild-type and mutated PA28γ genes and the transgene encoding the HCV core protein under the control of the HBV X promoter were investigated. Positions corresponding to the screening primers and sizes of PCR products are shown. PCR products of the HCV core gene as well as wild-type and mutated PA28γ alleles were amplified from the genomic DNAs of PA28$\gamma^{-/-}$, PA28$\gamma^{+/+}$CoreTg, PA28$\gamma^{-/-}$, and PA28$\gamma^{-/-}$CoreTg mice. (*B*) Body weights of PA28$\gamma^{+/+}$, PA28$\gamma^{+/+}$CoreTg, PA28$\gamma^{-/-}$CoreTg, and PA28$\gamma^{-/-}$ mice at the age of 6 months. (*C*) HCV core protein levels in the livers of PA28$\gamma^{+/-}$CoreTg and PA28$\gamma^{-/-}$CoreTg mice were determined by ELISA (mean ± SD, n = 10). (*D*) Localization of HCV core protein in the liver. Liver sections of PA28$\gamma^{+/+}$, PA28$\gamma^{+/+}$CoreTg, and PA28$\gamma^{-/-}$CoreTg mice at the age of 2 months were stained with anti-HCV core antibody.

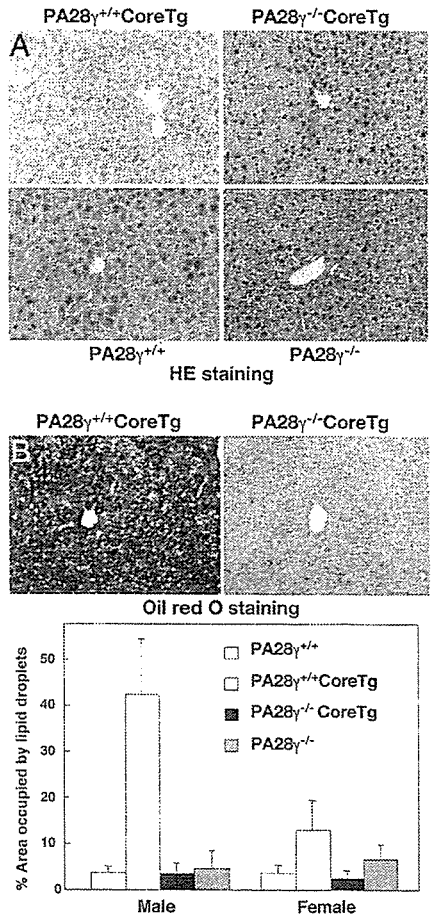

Fig. 2. Accumulation of lipid droplets by expression of HCV core protein. (*A*) Liver sections of the mice at the age of 6 months were stained with hematoxylin/eosin (HE). (*B*) (*Upper*) Liver sections of PA28$\gamma^{+/-}$CoreTg and PA28$\gamma^{-/-}$CoreTg mice at the age of 6 months were stained with oil red O. (*Lower*) The area occupied by lipid droplets of PA28$\gamma^{+/+}$ (white), PA28$\gamma^{+/+}$CoreTg (gray), PA28$\gamma^{-/-}$CoreTg (black), and PA28$\gamma^{-/-}$ (dark gray) mice was calculated by Image-Pro software (MediaCybernetics, Silver Spring, MD) (mean ± SD, n = 10).

appreciable abnormalities in all tissues examined, with the exception of a slight retardation of growth (22). HCV core gene-transgenic (PA28$\gamma^{+/+}$CoreTg) mice were bred with PA28$\gamma^{-/-}$ mice to create PA28$\gamma^{+/-}$CoreTg mice. The PA28$\gamma^{+/-}$CoreTg offspring were bred with each other, and PA28$\gamma^{-/-}$CoreTg mice were selected by PCR using primers specific to the target sequences (Fig. 1*A*). No significant differences in body weight were observed among the 6-month-old mice, although PA28$\gamma^{-/-}$ mice exhibited a slight retardation of growth (Fig. 1*B*). A similar level of PA28γ expression was detected in PA28$\gamma^{+/+}$CoreTg and PA28$\gamma^{+/+}$ mice (see Fig. 5*B*). The expression levels and molecular size of HCV core protein were similar in the livers of PA28$\gamma^{+/+}$CoreTg and PA28$\gamma^{-/-}$CoreTg mice (Fig. 1*C*; see also Fig. 5*B*).

PA28γ Is Required for Degradation of HCV Core Protein in the Nucleus and Induction of Liver Steatosis. HCV core protein has been detected at various sites, such as the endoplasmic reticulum, mitochondria, lipid droplets, and nucleus of cultured cell lines, as well as in hepatocytes of PA28$\gamma^{+/+}$CoreTg mice and hepatitis C patients (6, 23, 24). Although HCV core protein is predominantly detected in the cytoplasm of the liver cells of PA28$\gamma^{+/+}$CoreTg mice, as reported in ref. 6, in the present study a clear accumulation of HCV core protein was observed in the liver cell nuclei of PA28$\gamma^{-/-}$CoreTg mice (Fig. 1*D*). These findings clearly indicate that at least some fraction of the HCV core protein is translocated into the nucleus and is degraded through a PA28γ-dependent pathway. Mild vacuolation was observed in the cytoplasm of the liver cells of 4-month-old PA28$\gamma^{+/+}$CoreTg mice, and it became more severe at 6 months, as reported in ref. 25. Hematoxylin/eosin-stained liver sections of 6-month-old PA28$\gamma^{-/+}$CoreTg mice exhibited severe vacuolating lesions (Fig. 2*A*), which were clearly stained with oil red O (Fig. 2*B Upper*), whereas no such lesions were detected in the livers of PA28$\gamma^{-/-}$CoreTg, PA28$\gamma^{+/+}$, or PA28$\gamma^{-/-}$ mice at the same age. The areas occupied by the lipid droplets in the PA28$\gamma^{-/+}$CoreTg mouse livers were ≈10 and 2–4 times larger than those of male and female of PA28$\gamma^{+/+}$, PA28$\gamma^{-/-}$, and PA28$\gamma^{-/-}$CoreTg mice, respectively (Fig. 2*B Lower*). These results suggest that PA28γ is required for the induction of liver steatosis by HCV core protein in mice.

PA28γ Is Required for the Up-Regulation of SREBP-1c Transcription by HCV Core Protein in the Mouse Liver. To clarify the effects of a knockout of the PA28γ gene in PA28$\gamma^{+/-}$CoreTg mice on lipid

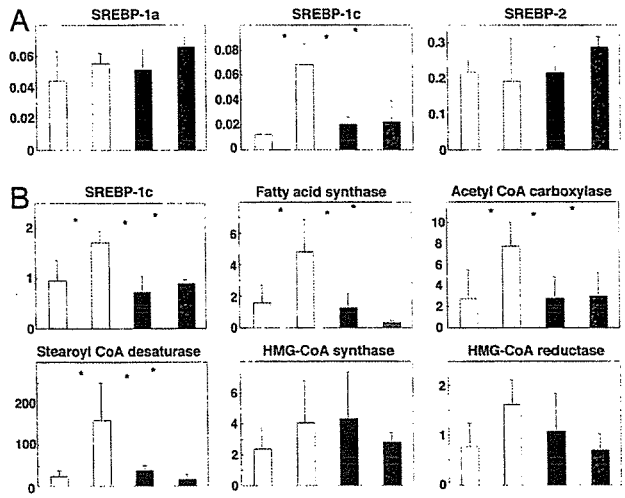

Fig. 3. Transcription of genes regulating lipid biosynthesis in the mouse liver. (*A*) Total RNA was prepared from the livers of 2-month-old mice; and the transcription of genes encoding SREBP-1a, SREBP-1c, and SREBP-2 was determined by real-time PCR. (*B*) The transcription of genes encoding SREBP-1c, fatty acid synthase, acetyl-CoA carboxylase, stearoyl-CoA desaturase, HMG-CoA synthase, and HMG-CoA reductase of 6-month-old mice was measured by real-time PCR. The transcription of the genes was normalized with that of hypoxanthine phosphoribosyltransferase, and the values are expressed as relative activity ($n = 5$; *, $P < 0.05$; **, $P < 0.01$). The transcription of each gene in PA28$\gamma^{+/+}$, PA28$\gamma^{-/-}$CoreTg, PA28$\gamma^{-/-}$CoreTg, and PA28$\gamma^{-/-}$ mice is indicated by white, gray, black, and dark gray bars, respectively.

metabolism, genes related to the lipid biosyntheses were examined by real-time quantitative PCR. Transcription of SREBP-1c was higher in the livers of PA28$\gamma^{+/+}$CoreTg mice than in those of PA28$\gamma^{+/+}$, PA28$\gamma^{-/-}$, and PA28$\gamma^{-/-}$CoreTg mice at 2 months of age, but no such increases in SREBP-2 and SREBP-1a were observed (Fig. 3*A*). Although transcription of SREBP-1c and its regulating enzymes, such as acetyl-CoA carboxylase, fatty acid synthase, and stearoyl-CoA desaturase, was also enhanced in the livers of 6-month-old PA28$\gamma^{+/+}$CoreTg mice compared with the levels in the livers of PA28$\gamma^{+/+}$, PA28$\gamma^{-/-}$, and PA28$\gamma^{-/-}$CoreTg mice, no statistically significant differences were observed with respect to the transcription levels of cholesterol biosynthesis-related genes that are regulated by SREBP-2 (e.g., HMG-CoA synthase and HMG-CoA reductase) (Fig. 3*B*). These results suggest the following: (*i*) the up-regulation of SREBP-1c transcription in the livers of mice requires both HCV core protein and PA28γ; and (*ii*) the nuclear accumulation of HCV core protein alone, which occurs because of the lack of degradation along a PA28γ-dependent proteasome pathway, does not activate the *srebp-1c* promoter.

HCV Core Protein Indirectly Potentiates *srebp-1c* Promoter Activity in an LXRα/RXRα-Dependent Manner. LXRα, which is primarily expressed in the liver, forms a complex with RXRα and synergistically potentiates *srebp-1c* promoter activity (16). Activation of RXRα by HCV core protein suggests that cellular fatty acid synthesis is modulated by the SREBP-1c pathway, although HCV core protein was not included in the transcription factor complex in the electrophoresis mobility shift assay (EMSA) (17). To analyze the effect of HCV core protein and PA28γ on the activation of the *srebp-1c* promoter, we first examined the effect of HCV core protein on the binding of the LXRα/RXRα complex to the LXR-response element (LXRE) located upstream of the SREBP-1c gene (Fig. 4*A*). Although a weak shift of the labeled LXRE probe was observed by incubation with nuclear extracts prepared from 293T cells expressing FLAG-tagged LXRα and HA-tagged RXRα, a clear shift was obtained by the treatment of cells with 9-*cis*-retinoic acid and 22(*R*)-hydroxylcholesterol, ligands for LXRα and RXRα, respectively. In contrast, coexpression of HCV core protein with LXRα and RXRα potentiated the shift of the probe irrespective of the treatment with the ligands. Addition of 500 times the amount of nonlabeled LXRE probe (competitor) diminished the shift of the labeled probe induced by the ligands and/or HCV core protein. Furthermore, coincubation of the nuclear fraction with antibody to FLAG or HA tag but not with antibody to either HCV core or PA28γ caused a supershift of the labeled probe. These results indicate that HCV core protein does not participate in the LXRα/RXRα–LXRE complex but indirectly enhances the binding of LXRα/RXRα to the LXRE.

The activity of the *srebp-1c* promoter was enhanced by the expression of HCV core protein in 293T cells, and it was further enhanced by coexpression of LXRα/RXRα (Fig. 4*B*). Enhancement of the *srebp-1c* promoter by coexpression of HCV core protein and LXRα/RXRα was further potentiated by treatment with the ligands for LXRα and RXRα. The cells treated with 9-*cis*-retinoic acid exhibited more potent enhancement of the *srebp-1c* promoter than those treated with 22(*R*)-hydroxylcholesterol. HCV core protein exhibited more potent enhancement of the *srebp-1c* promoter in cells treated with both ligands than in those treated with either ligand alone. These results suggest that HCV core protein poten-

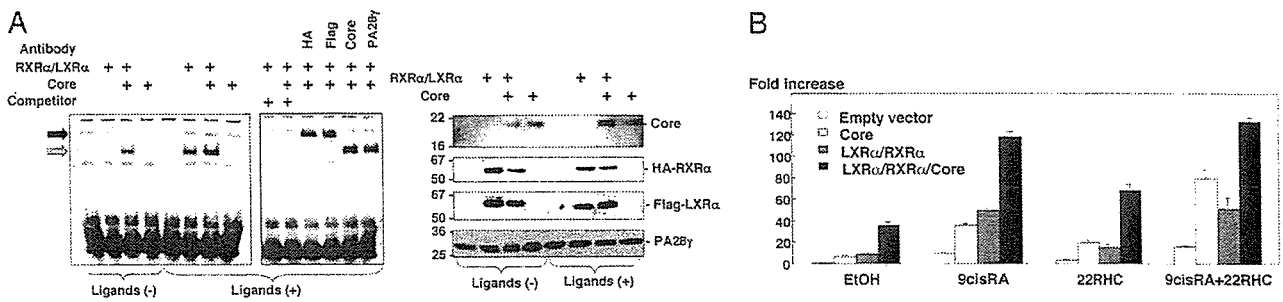

Fig. 4. Activation of the *srebp-1c* promoter by HCV core protein. (*A*) FLAG-LXRα and HA-RXRα were expressed in 293T cells together with or without HCV core protein. Ligands for LXRα and RXRα dissolved in ethanol [Ligands (+)] or ethanol alone [Ligands (−)] were added to the culture supernatant at 24 h posttransfection. Cells were harvested at 48 h posttransfection, and nuclear extracts were mixed with the reaction buffer for EMSA in the presence or absence of antibody (100 ng) against HA, FLAG, HCV core or PA28γ, or nonlabeled LXRE probe (Competitor). (*Left*) The resulting mixtures were subjected to PAGE and blotted with horseradish peroxidase/streptavidin. The mobility shift of the LXRE probe and its supershift are indicated by a gray and black arrow, respectively. (*Right*) Expression of HCV core, HA-RXRα, FLAG-LXRα, and PA28γ in cells was detected by immunoblotting. (*B*) Effects of ligands for RXRα, 9-*cis*-retinoic acid (9cisRA), and for LXRα, 22(*R*)-hydroxylcholesterol (22RHC), on the activation of the *srebp-1c* promoter in 293T cells expressing RXRα, LXRα, and/or HCV core protein. Ligands were added into the medium at 24 h posttransfection at a concentration of 5 μM, and the cells were harvested after 24 h of incubation.

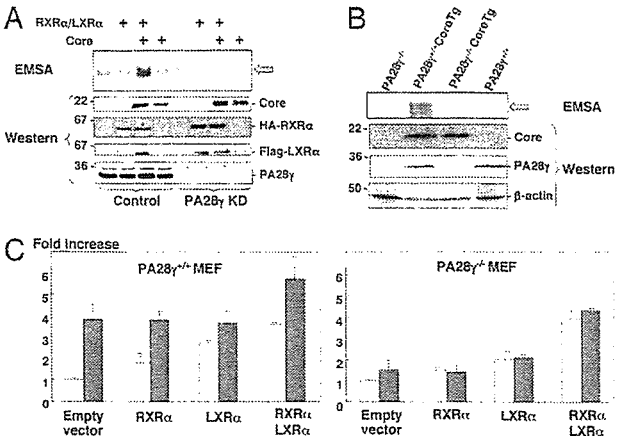

Fig. 5. PA28γ is required for HCV core-dependent activation of the *srebp-1c* promoter. (*A*) Effect of PA28γ knockdown on the LXRα/RXRα–DNA complex. FLAG-LXRα and HA-RXRα were expressed in FLC4 (control) or PA28γ-knockdown (PA28γ KD) cells together with or without HCV core protein. Cells were harvested at 48 h posttransfection, and nuclear extracts were mixed with the reaction buffer for EMSA. (*Upper*) The resulting mixtures were subjected to PAGE and blotted with horseradish peroxidase-streptavidin. The mobility shift of the LXRE probe is indicated by an arrow. (*Lower*) Expression of HCV core, HA-RXRα, FLAG-LXRα, and PA28γ in cells was detected by immunoblotting. (*B*) Effect of PA28γ knockout on the LXRα/RXRα–DNA complex in the mouse liver. (*Upper*) Nuclear extracts were prepared from the livers of 2-month-old PA28γ$^{-/-}$, PA28γ$^{+/+}$CoreTg, PA28γ$^{-/-}$CoreTg, and PA28γ$^{+/+}$ mice and subjected to EMSA. The mobility shift of the LXRE probe is indicated by an arrow. (*Lower*) The expression of HCV core, PA28γ, and β-actin in the livers of the mice was detected by immunoblotting. (*C*) Effect of HCV core protein on *srebp-1* promoter activity in PA28γ-knockout fibroblasts. A plasmid encoding firefly luciferase under the control of the *srebp-1c* promoter was transfected into MEFs prepared from PA28γ$^{+/+}$ (*Left*) or PA28γ$^{-/-}$ (*Right*) mice together with a plasmid encoding a *Renilla* luciferase. An empty plasmid or plasmids encoding mouse RXRα or LXRα were also cotransfected into the cells together with (gray bars) or without (white bars) a plasmid encoding HCV core protein. Luciferase activity under the control of the *srebp-1c* promoter was determined, and it is expressed as the fold increase in relative luciferase activity after standardization with the activity of *Renilla* luciferase.

tiates *srebp-1c* promoter activity in an LXRα/RXRα-dependent manner.

HCV Core Protein Activates the *srepb-1c* Promoter in an LXRα/RXRα- and PA28γ-Dependent Manner. To examine whether PA28γ is required for HCV core-induced enhancement of *srebp-1c* promoter activity in human liver cells, a PA28γ-knockdown human hepatoma cell line (FLC4 KD) was prepared. Enhancement of binding of the LXRE probe to LXRα/RXRα by coexpression of HCV core protein and LXRα/RXRα in FLC4 cells was diminished by knockdown of the PA28γ gene (Fig. 5*A*). Furthermore, formation of the LXRα/RXRα–LXRE complex was enhanced in the livers of PA28γ$^{+/+}$CoreTg mice but not in those of PA28γ$^{-/-}$, PA28γ$^{+/+}$, or PA28γ$^{-/-}$CoreTg mice (Fig. 5*B*). The expression of the HCV core protein in the mouse embryonic fibroblasts (MEFs) of PA28γ$^{+/+}$ mice induced the activation of the mouse *srebp-1c* promoter through the endogenous expression of LXRα and RXRα (Fig. 5*C Left*). Further enhancement of the activation of the *srebp-1c* promoter by HCV core protein in PA28γ$^{+/+}$ MEFs was achieved by the exogenous expression of both LXRα and RXRα. However, no enhancing effect of HCV core protein on *srebp-1c* promoter activity was observed in PA28γ$^{-/-}$ MEFs (Fig. 5*C Right*). These results support the notion that HCV core protein enhances the activity of the *srepb-1c* promoter in an LXRα/RXRα- and PA28γ-dependent manner.

Table 1. HCC in mice at 16–18 months of age

Mouse and sex	Total no. of mice	No. of mice developing HCC	Incidence, %
PA28γ$^{+/+}$CoreTg			
Male	17	5	29.4
Female	28	3	10.7
PA28γ$^{+/-}$			
Male	16	0	0
Female	4	0	0
PA28γ$^{-/-}$			
Male	23	0	0
Female	13	0	0
PA28γ$^{-/-}$CoreTg			
Male	15	0	0
Female	21	0	0

PA28γ Plays a Crucial Role in the Development of HCC in PA28γ$^{+/+}$ CoreTg Mice. The incidence of hepatic tumors in male PA28γ$^{+/+}$ CoreTg mice older than 16 months was significantly higher than that in age-matched female PA28γ$^{+/+}$CoreTg mice (6). We reconfirmed here that the incidence of HCC in male and female PA28γ$^{+/+}$CoreTg mice at 16–18 months of age was 29.4% (5 of 17 mice) and 10.7% (3 of 28 mice), respectively. To our surprise, however, no HCC developed in PA28γ$^{-/-}$CoreTg mice (males, 15; females, 21), although, as expected, no HCC was observed in PA28γ$^{+/-}$ (males, 16; females, 4) and PA28γ$^{-/-}$ mice (males, 23; females, 13) (Table 1). These results clearly indicate that PA28γ plays an indispensable role in the development of HCC induced by HCV core protein.

Discussion

HCV core protein is detected in the cytoplasm and partially in the nucleus and mitochondria of culture cells and hepatocytes of transgenic mice and hepatitis C patients (6, 23, 24, 26). Degradation of HCV core protein was enhanced by deletion of the C-terminal transmembrane region through a ubiquitin/proteasome-dependent pathway (27). We previously reported (18) that PA28γ binds directly to HCV core protein and then enhances degradation of HCV core protein in the nucleus through a proteasome-dependent pathway because HCV core protein was accumulated in nucleus of human cell line by treatment with proteasome inhibitor MG132. In this work, accumulation of HCV core protein was observed in nucleus of hepatocytes of PA28γ$^{-/-}$CoreTg mice (Fig. 1*D*). This result directly demonstrates that HCV core protein migrates into the nucleus and is degraded through a PA28γ-dependent pathway. However, HCV core protein accumulated in the nucleus because knockout of PA28γ gene abrogated the ability to cause liver pathology, suggesting that interaction of HCV core protein with PA28γ in the nucleus is prerequisite for the liver pathology induced by HCV core protein. We have previously shown (18) that HCV core protein is degraded through a PA28γ-dependent pathway, and Minami *et al.* (28) reported that PA28γ has a cochaperone activity with Hsp90. Therefore, degradation products of HCV core protein by means of PA28γ-dependent processing or correct folding of HCV core protein through cochaperone activity of PA28γ might be involved in the development of liver pathology. We do not know the reason why knockout of the PA28γ gene does not affect the total amount of HCV core protein in the liver of the transgenic mice. PA28γ-dependent degradation of HCV core protein may be independent of ubiquitination, as shown in SRC-3 (21), whereas knockdown of PA28γ in a human hepatoma cell line enhanced the ubiquitination of HCV core protein [supporting information (SI) Fig. 6], suggesting that lack of PA28γ suppresses a ubiquitin-independent degradation but enhances a ubiquitin-dependent degradation of HCV core protein. Therefore, the total amount of HCV

core protein in the liver of the mice may be unaffected by the knockout of the PA28γ gene.

Our results suggest that the interaction of HCV core protein with PA28γ leads to the activation of the *srebp-1c* promoter along an LXRα/RXRα-dependent pathway and the development of liver steatosis and HCC. HCV core protein was not included in the LXRα/RXRα–LXRE complex (Fig. 3*A*), suggesting that HCV core protein indirectly activates the *srebp-1c* promoter. Cytoplasmic HCV core protein was shown to interact with Sp110b, which is a transcriptional corepressor of RARα-dependent transcription, and this interaction leads to the sequestering of Sp110b in the cytoplasm, resulting in the activation of RARα-dependent transcription (29). The sequestration of an unidentified corepressor of the LXRα/RXRα heterodimer in the cytoplasm by HCV core protein may also contribute to the activation of the *srebp-1c* promoter. Although the precise physiological function of PA28γ-proteasome activity in the nucleus is not known, PA28γ has previously been shown (21) to regulate nuclear hormone receptors by means of the degradation of its coactivator SRC-3 and to participate in the fully Hsp90-dependent protein refolding (28). It appears reasonable to speculate that degradation or refolding of HCV core protein in a PA28γ-dependent pathway might be involved in the modulation of transcriptional regulators of various promoters, including the *srebp-1c* promoter. Saturated or monounsaturated fatty acids have been shown to enhance HCV RNA replication in Huh7 cells containing the full-length HCV replicon (7). The up-regulation of fatty acid biosynthesis by HCV core protein may also contribute to the efficient replication of HCV and to the progression of HCV pathogenesis.

Expression of HCV core protein was reported to enhance production of reactive oxygen species (ROS) (30), which leads to carbonylation of intracellular proteins (31). Enhancement of ROS production may trigger double-stranded DNA breaks and result in the development of HCC (30, 32, 33). HCV core protein could enhance the protein carbonylation in the liver of the transgenic mice in the presence but not in the absence of PA28γ (SI Fig. 7), suggesting that PA28γ is required for ROS production induced by HCV core protein. Development of HCC was observed in PA28γ$^{+/+}$CoreTg mice but not in PA28γ$^{-/-}$CoreTg mice (Table 1). Enhancement of ROS production by HCV core protein in the presence of PA28γ might be involved in the development of HCC in PA28γ$^{+/+}$CoreTg mice.

It is well known that resistant viruses readily emerge during the treatment with antiviral drugs targeting the viral protease or replicase, especially in the case of infection with RNA viruses. Therefore, antivirals targeting the host factors that are indispensable for the propagation of viruses might be an ideal target for the development of antiviral agents because of a lower rate of mutation than that of viral genome, if they have no side effects to patients. Importantly, the amino acid sequence of PA28γ of mice is identical to that of human, and mouse PA28γ is dispensable because PA28γ knockout mice exhibit no abnormal phenotype except for mild growth retardation. Therefore, PA28γ might be a promising target for an antiviral treatment of chronic hepatitis C with negligible side effects.

In summary, we observed that a knockout of the PA28γ gene from PA28γ$^{+/+}$CoreTg mice induced the accumulation of HCV core protein in the nucleus and disrupted the development of both steatosis and HCC. Activation of the *srebp-1c* promoter was up-regulated by HCV core protein both *in vitro* and *in vivo* through a PA28γ-dependent pathway, suggesting that PA28γ plays a crucial role in the development of liver pathology induced by HCV infection.

Materials and Methods

Histology and immunohistochemistry, real-time PCR, and detection of proteins modified by ROS are discussed in *SI Materials and Methods*.

Plasmids and Reagents. Human PA28γ cDNA was isolated from a human fetal brain library (18). The gene encoding HCV core protein was amplified from HCV strain J1 (genotype 1b) (34) and cloned into pCAG-GS (35). Mouse cDNAs of RXRα and LXRα were amplified by PCR from the total cDNAs of the mouse liver. The RXRα and LXRα genes were introduced into pEF-FLAGGspGBK (36) and pcDNA3.1 (Invitrogen, Carlsbad, CA), respectively. The targeting fragment for human PA28γ knockdown (GGATCCGGTGGATCAGGAAGTGAAGTTCAAGAGA-CTTCACTTCCTGATCCACCTTTTTTGGAAAAGCTT) was introduced into the BamHI and HindIII sites of pSilencer 4.1 U6 hygro vector (Ambion, Austin, TX). Mouse anti-FLAG (M2) and mouse anti-β-actin antibodies were purchased from Sigma (St. Louis, MO). Rabbit polyclonal antibody against synthetic peptides corresponding to amino acids 70–85 of PA28γ was obtained from AFFINITI (Exeter, U.K.). Horseradish peroxidase-conjugated goat anti-mouse and anti-rabbit IgGs were purchased from ICN Pharmaceuticals (Aurora, OH). Rabbit anti-HCV core protein was prepared by immunization with recombinant HCV core protein (amino acids 1-71), as described in ref. 24. Mouse monoclonal antibody to HCV core protein was kindly provided by S. Yagi (37). The plasmid for expression of HA-tagged ubiquitin was described in ref. 27.

Preparation of PA28γ-Knockout HCV CoreTg Mice. The generation of C57BL/6 mice carrying the gene encoding HCV core protein genotype 1b line C49 and that of PA28γ$^{-/-}$ mice have been reported previously (22, 25). Both strains were crossbred with each other to create PA28γ$^{-/-}$CoreTg mice. PA28γ$^{-/-}$CoreTg mice were identified by PCR targeted at the PA28γ or HCV core gene (22, 25). Using 1 μg of genomic DNA obtained from the mouse tail, the PA28γ gene was amplified by PCR with the following primers: sense, PA28-3 (AGGTGGATCAGGAAGTGAAGCTCAA); and antisense, PA28γ-5cr (CACCTCACTTGTGATCCGCTCTCT-GAAAGAATCAACC). The targeted sequence for the PA28γ-knockout mouse was detected by PCR using the PA28-3 primer and the PAKO-4 primer (TGCAGTTCATTCAGGGCACCGGA-CAG). The transgene encoding HCV core protein was detected by PCR as described in ref. 25. The expression of PA28γ and HCV core protein in the livers of 6-month-old mice was confirmed by Western blotting with mouse monoclonal antibody to HCV core protein, clone 11-10, and rabbit antibody to PA28γ. Mice were cared for according to the institutional guidelines. The mice were given ordinary feed, CRF-1 (Charles River Laboratories, Yokohama, Japan), and they were maintained under specific pathogen-free conditions.

All animal experiments conformed to the Guidelines for the Care and Use of Laboratory Animals, and they were approved by the Institutional Committee of Laboratory Animal Experimentation (Research Institute for Microbial Diseases, Osaka University).

Preparation of Mouse Embryonic Fibroblasts. MEFs were prepared as described in ref. 22. MEFs were cultured at 37°C under an atmosphere of 5% CO_2 in Dulbecco's modified Eagle's medium (Sigma) supplemented with 10% FBS, penicillin, streptomycin, sodium pyruvate, and nonessential amino acids.

Transfection and Immunoblotting. Plasmid vectors were transfected into the MEFs and 293T cells by liposome-mediated transfection by using Lipofectamine 2000 (Invitrogen). The amount of HCV core protein in the liver tissues was determined by an ELISA as described in ref. 37. The cell lysates were subjected to SDS/PAGE (12.5% gel), and they were then transferred onto PVDF membranes. Proteins on the membranes were treated with specific antibody and Super Signal Femto (Pierce, Rockford, IL). The results were then visualized by using an LAS3000 imaging system (Fuji Photo Film, Tokyo, Japan). The method of immunoprecipitation test is described in ref. 18.

Reporter Assay for *srebp-1c* Promoter Activity. The genomic DNA fragment encoding the *srebp-1c* promoter region (located from residues −410 to +24) was amplified from a mouse genome. The fragment was introduced into the KpnI and HindIII sites of pGL3-Basic (Promega, Madison, WI), and it was designated as pGL3-srebp-1cPro. The plasmids encoding RXRα and LXRα were transfected into MEFs together with pGL3-srebp-1cPro and a control plasmid encoding *Renilla* luciferase (Promega). The total DNA for transfection was normalized by the addition of empty plasmids. Cells were harvested at 24 h posttransfection. The ligand of RXRα, 9-*cis*-retinoic acid (Sigma), and that of LXRα, 22(*R*)-hydroxylcholesterol (Sigma) were added at a final concentration of 5 μM each to the culture medium of 293T cells transfected with pGL3-srebp-1cPro together with expression plasmids encoding RXRα, LXRα, and HCV core protein at 24 h posttransfection. Cells were harvested 24 h after treatment. Luciferase activity was measured by using the dual-luciferase reporter assay system (Promega). Firefly luciferase activity was standardized with that of *Renilla* luciferase, and the results are expressed as the fold increase in relative luciferase units.

Electrophoresis Mobility Shift Assay (EMSA). EMSA was carried out by using a LightShift Chemiluminescent EMSA kit (Pierce) according to the manufacturer's protocol. Nuclear extract of the cell lines and liver tissue was prepared with an NE-PER nuclear and cytoplasmic extraction reagent kit (Pierce). Briefly, double-stranded oligonucleotides for EMSA were prepared by annealing both strands of each LXRE of the *srebp-1c* promoter (5′-GGACGCCCGCTAGTAACCCCGGC-3′) (16). Both strands were labeled at the 5′ ends with biotin. The annealed probe was incubated for 20 min on ice with nuclear extract (3 μg of protein) in a reaction buffer containing 10 mM Tris·HCl (pH 7.5), 50 mM KCl, 1 mM DTT, 0.05 μg/μl poly(dI-dC), 2.5% glycerol, 0.05% Nonidet P-40, and 0.1 nM labeled probe, with or without 1 mM nonlabeled probe. The resulting mixture was subjected to PAGE (5% gel) at 120 V for 30 min in 0.5× TBE. The DNA–protein complex was transferred to a Hybond N+ membrane (Amersham, Piscataway, NJ), incubated with horseradish peroxidase-conjugated streptavidin, and visualized by using an LAS3000 imaging system.

Statistical Analysis. The results are expressed as the mean ± SD. The significance of differences in the means was determined by Student's *t* test.

We thank H. Murase for secretarial work and D. C. S. Huang for providing the plasmids. This work was supported in part by grants-in-aid from the Ministry of Health, Labor, and Welfare; the Ministry of Education, Culture, Sports, Science, and Technology; the 21st Century Center of Excellence Program; and the Foundation for Biomedical Research and Innovation.

1. Wasley A, Alter MJ (2000) *Semin Liver Dis* 20:1–16.
2. Bach N, Thung SN, Schaffner F (1992) *Hepatology* 15:572–577.
3. Lefkowitch JH, Schiff ER, Davis GL, Perrillo RP, Lindsay K, Bodenheimer HC, Jr., Balart LA, Ortego TJ, Payne J, Dienstag JL, *et al.* (1993) *Gastroenterology* 104:595–603.
4. Barba G, Harper F, Harada T, Kohara M, Goulinet S, Matsuura Y, Eder G, Schaff Z, Chapman MJ, Miyamura T, Brechot C (1997) *Proc Natl Acad Sci USA* 94:1200–1205.
5. Hope RG, McLauchlan J (2000) *J Gen Virol* 81:1913–1925.
6. Moriya K, Fujie H, Shintani Y, Yotsuyanagi H, Tsutsumi T, Ishibashi K, Matsuura Y, Kimura S, Miyamura T, Koike K (1998) *Nat Med* 4:1065–1067.
7. Kapadia SB, Chisari FV (2005) *Proc Natl Acad Sci USA* 102:2561–2566.
8. Su AI, Pezacki JP, Wodicka L, Brideau AD, Supekova L, Thimme R, Wieland S, Bukh J, Purcell RH, Schultz PG, Chisari FV (2002) *Proc Natl Acad Sci USA* 99:15669–15674.
9. Wang C, Gale M, Jr, Keller BC, Huang H, Brown MS, Goldstein JL, Ye J (2005) *Mol Cell* 18:425–434.
10. Horton JD, Shimomura I, Brown MS, Hammer RE, Goldstein JL, Shimano H (1998) *J Clin Invest* 101:2331–2339.
11. Pai JT, Guryev O, Brown MS, Goldstein JL (1998) *J Biol Chem* 273:26138–26148.
12. Shimano H, Horton JD, Hammer RE, Shimomura I, Brown MS, Goldstein JL (1996) *J Clin Invest* 98:1575–1584.
13. Shimano H, Horton JD, Shimomura I, Hammer RE, Brown MS, Goldstein JL (1997) *J Clin Invest* 99:846–854.
14. Shimano H, Shimomura I, Hammer RE, Herz J, Goldstein JL, Brown MS, Horton JD (1997) *J Clin Invest* 100:2115–2124.
15. Repa JJ, Liang G, Ou J, Bashmakov Y, Lobaccaro JM, Shimomura I, Shan B, Brown MS, Goldstein JL, Mangelsdorf DJ (2000) *Genes Dev* 14:2819–2830.
16. Yoshikawa T, Shimano H, Amemiya-Kudo M, Yahagi N, Hasty AH, Matsuzaka T, Okazaki H, Tamura Y, Iizuka Y, Ohashi K, *et al.* (2001) *Mol Cell Biol* 21:2991–3000.
17. Tsutsumi T, Suzuki T, Shimoike T, Suzuki R, Moriya K, Shintani Y, Fujie H, Matsuura Y, Koike K, Miyamura T (2002) *Hepatology* 35:937–946.
18. Moriishi K, Okabayashi T, Nakai K, Moriya K, Koike K, Murata S, Chiba T, Tanaka K, Suzuki R, Suzuki T, *et al.* (2003) *J Virol* 77:10237–10249.
19. Masson P, Andersson O, Petersen UM, Young P (2001) *J Biol Chem* 276:1383–1390.
20. Li J, Rechsteiner M (2001) *Biochimie* 83:373–383.
21. Li X, Lonard D, Jung SY, Malovannaya A, Feng Q, Qin J, Tsai SY, Tsai M, O'Malley BW (2006) *Cell* 124:381–392.
22. Murata S, Kawahara H, Tohma S, Yamamoto K, Kasahara M, Nabeshima Y, Tanaka K, Chiba T (1999) *J Biol Chem* 274:38211–38215.
23. Falcon V, Acosta-Rivero N, Chinea G, Gavilondo J, de la Rosa MC, Menendez I, Duenas-Carrera S, Vina A, Garcia W, Gra B, *et al.* (2003) *Biochem Biophys Res Commun* 305:1085–1090.
24. Suzuki R, Sakamoto S, Tsutsumi T, Rikimaru A, Tanaka K, Shimoike T, Moriishi K, Iwasaki T, Mizumoto K, Matsuura Y, *et al.* (2005) *J Virol* 79:1271–1281.
25. Moriya K, Yotsuyanagi H, Shintani Y, Fujie H, Ishibashi K, Matsuura Y, Miyamura T, Koike K (1997) *J Gen Virol* 78:1527–1531.
26. Yasui K, Wakita T, Tsukiyama-Kohara K, Funahashi SI, Ichikawa M, Kajita T, Moradpour D, Wands JR, Kohara M (1998) *J Virol* 72:6048–6055.
27. Suzuki R, Tamura K, Li J, Ishii K, Matsuura Y, Miyamura T, Suzuki T (2001) *Virology* 280:301–309.
28. Minami Y, Kawasaki H, Minami M, Tanahashi N, Tanaka K, Yahara I (2000) *J Biol Chem* 275:9055–9061.
29. Watashi K, Hijikata M, Tagawa A, Doi T, Marusawa H, Shimotohno K (2003) *Mol Cell Biol* 23:7498–7509.
30. Machida K, Cheng KT, Lai CK, Jeng KS, Sung VM, Lai MM (2006) *J Virol* 80:7199–7207.
31. Nystrom T (2005) *EMBO J* 24:1311–1317.
32. Bromberg JF, Wrzeszczynska MH, Devgan G, Zhao Y, Pestell RG, Albanese C, Darnell JE, Jr (1999) *Cell* 98:295–303.
33. Carballo M, Conde M, El Bekay R, Martin-Nieto J, Camacho MJ, Monteseirin J, Conde J, Bedoya FJ, Sobrino F (1999) *J Biol Chem* 274:17580–17586.
34. Aizaki H, Aoki Y, Harada T, Ishii K, Suzuki T, Nagamori S, Toda G, Matsuura Y, Miyamura T (1998) *Hepatology* 27:621–627.
35. Niwa H, Yamamura K, Miyazaki J (1991) *Gene* 108:193–199.
36. Huang DC, Cory S, Strasser A (1997) *Oncogene* 14:405–414.
37. Aoyagi K, Ohue C, Iida K, Kimura T, Tanaka E, Kiyosawa K, Yagi S (1999) *J Clin Microbiol* 37:1802–1808.

Available online at www.sciencedirect.com
SCIENCE DIRECT®
Hepatology Research 32 (2005) 213–217
HEPATOLOGY RESEARCH
http://www.elsevier.com/locate/hepres

Changes in natural killer T cells subsets during therapy in type C hepatitis and hepatocellular carcinoma

Akihiko Okumura, Tetsuya Ishikawa, Tadashi Maeno, Ken Sato, Minoru Ayada, Naoki Hotta, Taeko Yamauchi, Yoshitaka Fukuzawa, Shinichi Kakumu *

Department of Internal Medicine, Division of Gastroenterology and Research Center for Infectious Disease, Aichi Medical University School of Medicine, 21 Karimata Yazako, Nagakute-cho, Aichi-gun, Aichi-ken 480-1195, Aichi, Japan

Received 21 December 2004; received in revised form 1 February 2005; accepted 24 February 2005
Available online 17 May 2005

Abstract

Natural killer T (NKT) cells share features of both classical T cells and NK cells. NKT are heterogenous populations, and recognize glycolipids associated with CD1d molecule. We investigated Th1/Th2 cytokine production as well as frequency and phenotype of circulating NKT cells in 14 healthy subjects and in patients during therapy with type C chronic hepatitis (CH; 14 cases) and hepatocellular carcinoma (HCC; 13 cases). Peripheral blood mononuclear cells (PBMC) were obtained before and 2 weeks later interferon (IFN)/ribavirin and radiofrequency ablation therapy for CH and HCC, respectively. PBMC were cultured for 10 days with α-galactosylceramide (α-GalCer) and interleukin-2 (IL-2). Frequencies and IFN-γ/IL-4 production of NKT cells were analyzed using flow cytometry. Intrahepatic lymphocytes were analyzed in seven CH patients with liver biopsy specimen. Prevalence of circulating Vα24+CD3+ T cells was 0.9 ± 0.9% of PBMC for controls and increased to 8.5 ± 8.9% ($p < 0.001$) in response to α-GalCel. Similar frequency and expansion were noted in CH. The frequency increased during therapy. The prevalence in HCC tended to be high compared to controls and response to α-GalCel was well. Although frequency of Vα24+Vβ11+CD3+ T cells was low in all groups, the distribution pattern was similar to Vα24+Vβ11−CD3+ T cells. Prevalence of CD56+CD3+ T cells was low independent of therapy in CH (2–3%) compared to 5.0 ± 4.0% of controls, although response to α-GalCel was not impaired. IFN-γ production of Vα24+CD3+ T cells did not differ among groups, but became greater after treatment in contrast to lowered IL-4 production. Frequencies of NKT populations were higher in liver than in peripheral blood. Our study suggests that CD1d-reactive T cells have distinct distribution in different populations and therapy for patients alters cytokine response of NKT cells.

Keywords: NKT cell; HCV-related disease; Therapy; Cytokine; α-Galactosylceramide

1. Introduction

Hepatitis C virus (HCV) is a positive strand RNA virus, which is the leading causative agent of chronic hepatitis (CH) [1]. There is no vaccine and the only treatment is interferon (IFN) therapy. It often progresses to liver cirrhosis and hepatocellular carcinoma (HCC). The host immune response to HCV antigens is thought to determine whether viral clearance or chronicity occurs. Chronicity of HCV infection is associated with weaker HCV-specific T cell responses that contribute to liver damage [2].

Natural killer T (NKT) cells are heterogenous populations, express T cell receptor (TCR) and recognize glycolipids associated with CD1d molecule [3–5]. Human Vα24 NKT cells can be activated by a synthetic glycolipid, α-galactosylceramide (α-GalCer) in a CD1d-dependent fashion, as can murine Vα14 NKT cells [6,7]. Activated NKT cells produce both interleukin-4 (IL-4) and IFN-γ and regulate Th1/Th2 cytokine response [8]. NKT cells appear to be involved in innate response against

Abbreviations: CH, chronic hepatitis; α-GalCer, α-galactosylceramide; HCC, hepatocellular carcinoma; HCV, hepatitis C virus; IFN, interferon; IL, interleukin; NKT, natural killer T

* Corresponding author. Tel.: +81 561 62 3311x2382; fax: +81 561 63 0796.
E-mail address: kakumu@aichi-med-u.ac.jp (S. Kakumu).

1386-6346/$ – see front matter © 2005 Elsevier B.V. All rights reserved.
doi:10.1016/j.hepres.2005.02.008

autoimmunity, infection and tumor in humans as well as in mice [9–12].

The human liver contains multiple populations of NKT cells with distinct activities [13]. NKT cells are suggested to contibute to destructive as well as protective immune responses in the liver infected with HCV [14,15], and α-GalCer exerts direct activity against hepatitis B and C viruses [16]. It is also indicated that the response of Vα24 NKT cells is impaired in cancer patients [17]. However, the role and function of NKT cells have been poorly understood during therapy in HCV-infected patients.

In the present study, we investigated the frequency and phenotype of circulating NKT cells during therapy in patients with type C CH and HCC. Simultaneously, we evaluated Th1/Th2 cytokine production (IFN-γ and IL-4) of NKT cells. In some with CH, intrahepatic distribution of NKT cells was studied with the tissue of liver biopsy.

2. Materials and methods

2.1. Patients

Fourteen patients with CH (9 males and 5 females with 54 ± 10 years; mean ± S.D.) and 13 patients with HCC (10 males and 3 females with 62 ± 9 years) were enrolled to the present study. As controls, 14 healthy subjects (10 males and 4 females with 48 ± 12 years) were selected without a clinical history of hepatitis and without symptoms or signs of liver disease. The diagnosis of CH and HCC was confirmed by liver biopsy and dynamic CT and/or celiac angiography, respectively. Based on Child-Pugh score, nine patients was diagnosed as grade A and four patients as grade B. All patients were seropositive for anti-HCV antibody as detected by a second-generation enzyme immunoassay test (Abbott Laboratories, North Chicago, IL) and the presence of HCV RNA was confirmed by Amplicore (Roche Diagnostic Inc., Tokyo). No patients had HBV infection; the diagnosis was made if patients had evidence of hepatitis B surface antigen (HBsAg). There was no serologic evidence of co-infection with other hepatotropic viruses. Other possible causes of chronic hepatitis (i.e. drug, alcohol, autoimmune and metabolic disorders) were excluded. All patients gave informed consent and the study was approved by the Human Studies Committee of Aichi Medical University School of Medicine.

2.2. Isolation of PBMC and IHMC

The blood was collected after obtaining informed consent from healthy volunteers and before and 2 weeks later IFN/ribavirin and radiofrequency ablation therapy for patients with CH and HCC, respectively. Peripheral blood mononuclear cells (PBMC) were separated from fresh heparinized peripheral blood by Conray–Ficoll density gradient centrifugation.

Liver tissue was obtained from liver biopsy before therapy in seven patients with CH. Liver specimens were cut into fine pieces and digested with 0.1% collagenase type IV in a flask with stirring at 37 °C for 10 min three times. Intrahepatic mononuclear cells (IHMC) were separated on Conray–Ficoll density gradient centrifugation.

The PBMC were cultured in 24-well plates (1×10^6 cells/well) for 10 days in 1 ml suspended in RPMI 1640 (GIBCO Laboratories, Grand Island, NY) culture medium containing 10% (v/v) heat-inactivated FBS, glutamine and antibiotics, in the presence of 10 ng/ml α-GalCer (KRN7000, Kirin Brewery Co., Tokyo) and 200 U/ml recombinant human IL-2 (Pharmingen, San Diego, CA).

2.3. Flow cytometric analysis

In this study, we defined NKT cells as cells with Vα24+, CD56+ in the fraction of CD3+ cells, and cells with both Vα24 and Vβ11 expression as described by others [12,13,17–19]. To detect NKT cells and intracellular cytokine production, three-color flow cytometry was done. Fresh PBMC (day 0) or cultured cells (day 10) were stained with phycoerythrin (PE)-conjugated anti-TCR Vα24 Ab (Pharmingen), fluorescein isothiocyanate (FITC)-conjugated anti-TCR Vβ11 Ab (Pharmingen), FITC-conjugated anti-CD56 Ab (Becton Dickinson, San Jose, CA), PE-conjugated anti-CD161 Ab (Becton Dickinson) and peridinium chlorphyll protein (Per CP)-conjugated anti-CD3 Ab (Becton Dickinson) on ice for 30 min, washed twice, fixed in PBS with 1% paraformaldehyde. Frequency and phenotype of NKT cells for IHMC were analyzed at day 0.

The simultaneous flow cytometric intracellular cytokine staining protocol was that described by Metelitsa with slight modifications [20], using FITC-conjugated anti-IFN-γ Ab (Pharmingen) and PE-conjugated anti-IL-4 Ab (Parmingen) and subsequent treatment in FACS Permeabilizing Solution (Becton Dickinson).

2.4. FACS analysis

The fixed samples were acquired on a FACS Calibur flow cytometer (Becton Dickinson) using CellQuest software (Becton Dickinson).

2.5. Statistical analysis

Results were presented as mean ± S.D. The significance of the differences between the groups was determined by the one-way factorial ANOVA. Correlation analysis was performed using Spearman's rank correlation test.

3. Results

Prevalence of circulating Vα24+CD3+ T cells was 0.9 ± 0.9% of PBMC for controls and increased to 8.5 ± 8.9% ($p < 0.001$) in cultures with α-GalCel for 10 days (Fig. 1). Similar frequency and expansion (from 1.1 ± 0.9 to

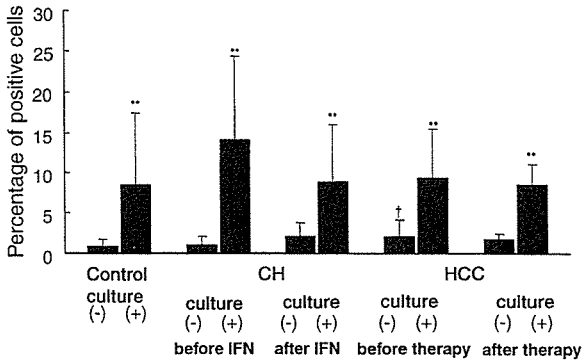

Fig. 1. Frequency of TCR Vα24+CD3+ T cells in peripheral blood mononuclear cells of healthy subjects and patients with type C chronic hepatitis (CH) and hepatocellular carcinoma (HCC) in the absence (−) or presence (+) of α-galactosylceramide and interleukin 2. p-Values in comparison with before and after culture: $^{**}p<0.01$; p-values in comparison with control and patient group before culture: $^{\dagger}p<0.05$.

14.0 ± 10.2% and $p<0.001$) were noted in patients with CH. Baseline frequency increased to 2.0 ± 1.9%, 2 weeks after start of combination therapy of IFN and ribavirin. In patients with HCC, the prevalence tended to be high (2.1 ± 2.0%) compared to controls, and response to α-GalCel was well (9.4 ± 6.0% and $p<0.001$). The frequency and response to α-GalCel after RFA therapy were not changed.

Although frequency of Vα24+Vβ11+CD3+ T cells was low (0.18 ± 0.17% for controls), the distribution pattern was similar to that of Vα24+CD3+ T cells and responded well to α-GalCel in both control and diseased groups (Fig. 2). Prevalence of CD56+CD3+ T cells was low independent of therapy in CH (2–3%) compared to 5.0 ± 4.0% of controls, although response to α-GalCel was not impaired (Fig. 3). In HCC, the prevalence was equivalent to controls while response to α-GalCel decreased.

IFN-γ production of Vα24+Vβ11−CD3+ T cells did not differ among groups (0.37 ± 0.67, 0.34 ± 0.51 and 0.20 ± 0.23% for controls, CH and HCC, respectively)

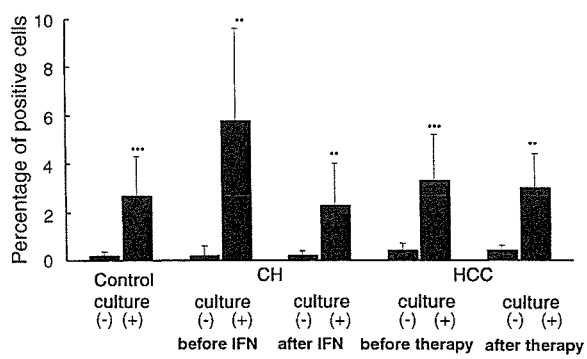

Fig. 2. Frequency of TCR Vα24+Vβ11+ T cells in peripheral blood mononuclear cells of healthy subjects and patients with type C chronic hepatitis (CH) and hepatocellular carcinoma (HCC) in the absence (−) or presence (+) of α-galactosylceramide and interleukin 2. p-Values in comparison with before and after culture: $^{**}p<0.01$ and $^{***}p<0.001$.

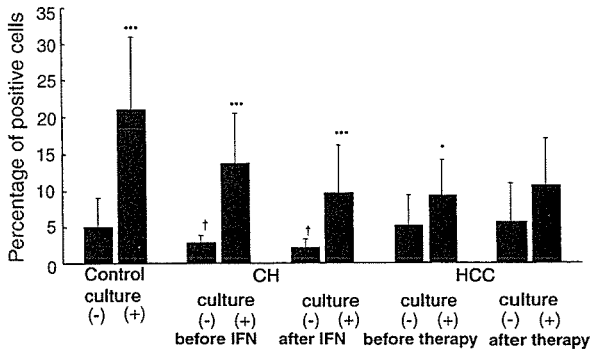

Fig. 3. Frequency of CD56+CD3+ T cells in peripheral blood mononuclear cells of healthy subjects and patients with type C chronic hepatitis (CH) and hepatocellular carcinoma (HCC) in the absence (−) or presence (+) of α-galactosylceramide and interleukin 2. p-Values in comparison with before and after culture: $^{*}p<0.05$ and $^{***}p<0.001$; p-values in comparison with control and patient group before culture: $^{\dagger}p<0.05$.

and became greater after treatment for CH (0.84 ± 0.72%) and HCC (0.90 ± 1.4%) (Fig. 4a). IL-4 production of Vα24+Vβ11−CD3+ T cells was lower in patients (0.65 ± 1.1 and 0.5 ± 0.6% for CH and HCC, respectively) than in controls (1.9 ± 2.3%) and the cytokine production was further suppressed by therapy for both CH and HCC as illustrated in Fig. 4b. Thus, Th1/Th2 ratio increased after therapy in both diseases. Frequencies of any NKT populations derived from patients with CH were significantly higher in liver than in peripheral blood, except for Vα24+CD3+ T cells because of wide range of distribution (Table 1).

There was no significant correlation between frequency and phenotype of NKT cells, and clinical and laboratory data including serum levels of alanine aminotranferase (ALT) and HCV RNA.

4. Discussion

Although much work has focused on the role of conventional antigen-specific T cell responses in HCV-infected patients, less is known regarding the role of other lymphocyte subsets including innate responses. A variety of NKT cells exist with different definitions [13,14,18–21]. Thus, it may be important to evaluate prevalence and function of CD1d-reactive NKT cell subsets such as CD56+, CD161+

Table 1
Distribution of NKT cells in intrahepatic and peripheral blood morionuclear cells from seven patients with chronic hepatitis C

	IHMC (%)	PBMC (%)	p-Value
CD3+CD56+	13.5 ± 4.6[a]	3.6 ± 3.0	<0.001
CD3+CD161+	26.3 ± 9.8	16.0 ± 7.2	<0.05
CD3+Vα24+	1.64 ± 2.71	0.94 ± 0.54	n.s.
Vα24+Vβll+	1.30 ± 2.41	0.05 ± 0.02	<0.05

IHMC, intrahepatic mononuclear cells; PBMC, peripheral blood mononuclear cells; n.s., not significant.
[a] Data are expressed as mean as ± S.D.

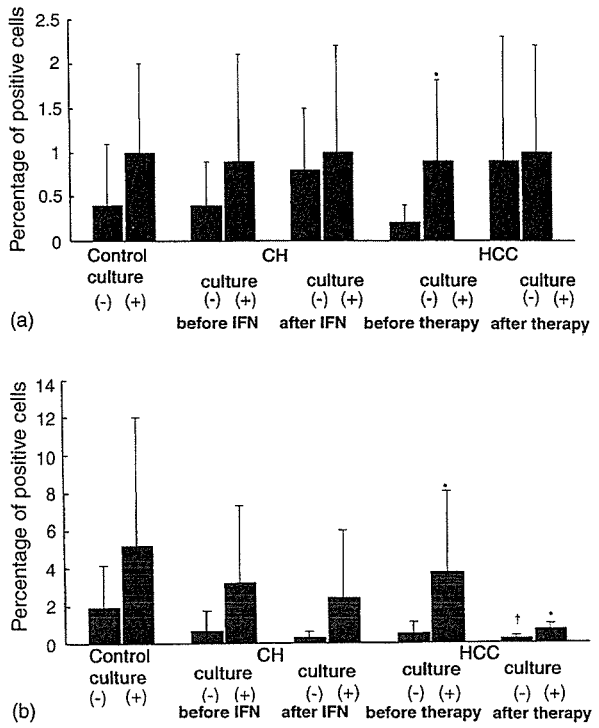

Fig. 4. (a) Frequency of IFN-γ+ cells among Vα24+CD3+ T cells in peripheral blood mononuclear cells of healthy subjects and patients with type C chronic hepatitis (CH) and hepatocellular carcinoma (HCC) in the absence (−) or presence (+) of α-galactosylceramide and interleukin 2. p-Values in comparison with before and after culture: $^{*}p < 0.05$. (b) Frequency of IL-4+ cells among Vα24+CD3+ T cells in peripheral blood mononuclear cells of healthy subjects and patients with type C chronic hepatitis and hepatocellular carcinoma in the absence (−) or presence (+) of α-galactosylceramide and interleukin 2. p-Values in comparison with before and after culture: $^{*}p < 0.05$; p-values in comparison with control and patient group before culture: $^{\dagger}p < 0.05$.

and Vα24+ T cells as well as Vα24/Vβ11 double-positive NKT cells in HCV-related disease.

Our present study showed that circulating Vα24+CD3+ T cells in patients with CH increased during IFN/ribavirin therapy. Although Vα24+CD3+ T cell is a small population (1–2%) of PBMC as indicated by our data and others, increased Vα24+CD3+ T cells may exert anti-viral and immunoregulatory function in the liver [14]. The mechanism involved in their activation in response to viral infection has yet to be determined [13,22,23]. In murine model, in vivo administration of α-GalCer induced a release of IFN-γ and suppressed of HBV replication [24]. Recently, others also reported that α-GalCer directly induced the innate host defense pathway resulting in direct activity for HBV and HCV [16].

Frequency of Vα24/Vβ11 double-positive NKT cells was very low in controls and diseased groups, but response to α-GalCer was well in all patients including HCC. Analysis of Vα24/Vβ11 double-positive NKT cells by others also revealed a low frequency of 0.01–0.14% in normal individuals and a similar range in HCV-infected patients [26]. The reason for this relatively high level of Vα24+ cells without an increased level of Vβ11+ cells is not clear. Surface phenotype and function of Vα24 single-positive cells may differ from that of Vα24/Vβ11 double-positive NKT cells. In man, since Vα24+Vβ11+CD3+ NKT cell is thought to be a representative phenotype of CD1d-restricted NKT cells [5–8], it is needed to analyze more its function and role regarding immunopathogenesis and response to therapy in HCV-related disease.

The prevalence of CD56+CD3+ T cells was low independent of therapy in CH compared to that of controls, although response to α-GalCer was not impaired. In contrast, response to α-GalCer decreased in HCC, while the prevalence was equivalent to controls. This finding suggests that CD56+ T cell is a distinct population from Vα24+ T cell regarding response to α-GalCer and phenotype. The lower level of CD56+ T cells observed in CH may be due to the down-regulation of TCR as a result of activation and apoptosis of the activated cells through a similar process [23,26]. Compartmentalization into the liver is also suggested [13,14]. Decreases in CD56+ T cells and Vα24+ T cells were noted in the liver with chronic HCV infection [19]. A decreased number of CD56+ T cells and NK cells in cirrhotic liver was suggested to be related to their susceptibility to HCC [27].

In the present study, IFN-γ production of Vα24+CD3+ T cells did not differ among each group, and it became greater after treatment for both CH and HCC, while IL-4 production became further lower after treatment in the patients. Thus, Th1/Th2 ratio increased after therapy in both diseases. Doherty et al. showed that the majority of CD56+CD3+ T cells in human liver produced inflammatory (Th1) cytokines only, while some Vα24 T cells simultaneously produced IFN-γ and IL-4 [13]. Exley et al. also revealed that IHL from chronic hepatitis C had high levels of CD161 and CD1d reactivity and CD1d-reative IHL were Th1 biased [14]. The others showed that CD1d-reactive invariant NKT cells produced IL-4, but they had diminished IFN-γ production in advanced cancer in contrast to our HCC patients who had relatively compensated liver function [28]. Collectively, these findings suggest that CD1d-reactive T cells may contribute to destructive as well as protective immune responses in the liver according to the circumstances of the host.

Alternatively, since we observed the response to α-GalCer by using PBMC, it may be difficult to analyze whether the response of various NKT cell subsets is direct action of α-GalCer or indirect action via cytokine. Thus it would be desirable to use individual NKT cell subsets.

In addition to the increased frequencies of different NKT populations, they are activated in the liver than in peripheral blood in humans and HCV-infected persons [13,14,25]. They may have distinct roles in immune response such as Th1 or Th2 biased dependent on the activity and stage of the disease.

In conclusion, our present study is preliminary. For example, it should be clarified how function of NKT cells is associated with clinical course of CH and how the function is related to the efficacy of combination therapy of IFN and ribavirin. Our data indicated increased IFN-γ production

after treatment in contrast to suppressed IL-4 production in HCC, suggesting the improvement of anti-tumor immunity in tumor-bearing host. However, we should be careful to interpret the finding because the mechanism of tumor immunity is more complexed. We have to clarify these subjects in the future study.

References

[1] Tong MJ, El-Farra NS, Reikes AR, Co RL. Clinical outcomes after transfusion-associated hepatitis C. N Engl J Med 1995;332:1463–6.

[2] Cerny A, Chisari FV. Pathogenesis of chronic hepatitis C: immunological features of hepatic injury and viral persistence. Hepatology 1999;30:595–601.

[3] Makino Y, Kanno R, Ito T, Higashino K, Taniguchi M. Predominant expression of invariant Vα14+ TCR α chain in NK1.1+ T cell populations. Int Immunol 1995;7:1157–61.

[4] Bendelac A, Rivera M, Park S, Roark J. Mouse CD1d-specific NK1 T cells: development, specificity, and function. Annu Rev Immunol 1997;15:535–62.

[5] Porcelli S, Modlin R. The CD1 system: antigen-presenting molecules for T cell recognition of lipids and glycolipids. Annu Rev Immunol 1999;17:297–329.

[6] Kawano T, Cui J, Koezuka Y, et al. CD1d-restricted and TCR-mediated activation of Vα14 NKT cells by glycosylceramides. Science 1997;278:1626–9.

[7] Spada F, Koezuka Y, Porcelli SA. CD1d-restricted recognition of synthetic glycolipid antigens by human natural killer T cells. J Exp Med 1998;188:1529–34.

[8] Vincent MS, Gumperz JE, Brenner MB. Understanding the function of CD1d-restricted T cells. Nat Immunol 2003;6:517–23.

[9] Kojo S, Adachi Y, Keino H, Taniguchi M, Sumida T. Dysfunction of T cell receptor Vα24Jα18+, Vβ11+ double-negative regulatory natural killer T cells in autoimmune diseases. Arthritis Rheum 2001;44:1127–36.

[10] Kita H, Imawari M, Gershwin ME. Cellular immune response in primary biliary cirrhosis. Hepatol Res 2004;28:12–7.

[11] Takeda K, Hayakawa Y, Van Kaer L, Matsuda H, Yagita H, Okumura K. Critical contribution of liver natural killer T cells to a murine model of hepatitis. Proc Natl Acad Sci USA 2000;97:5498–503.

[12] Kawano T, Nakayama T, Kamada N, et al. Antitumor cytotoxicity mediated by ligand-activated human Vα24 NKT cells. Cancer Res 1999;59:5102–5.

[13] Doherty DG, Norris S, Madrigal-Estebas L, et al. The human liver contains multiple populations of NK cells, T cells, and CD3+CD56+ natural T cells with distinct cytotoxic activities and Th1, Th2, and Th0 cytokine secretion patterns. J Immunol 1999;163:2314–21.

[14] Exley MA, He Q, Cheng O, et al. Compartmentalization of Th1-like noninvariant CD1d-reactive T cells in hepatitis C virus-infected liver. J Immunol 2002;168:1519–23.

[15] Poccia F, Agrati C. Intrahepatic natural immunity and HCV immunopathogenesis. Cell Death Differ 2003;10:S9–12.

[16] Mehta AS, Gu B, Conyers B, et al. α-Glycosylceramide and novel synthetic glycolipids directly induce the innate host defense pathway and have direct activity against hepatitis B and C viruses. Antimicrob Agent CH 2004;48:2085–90.

[17] Yanagisawa K, Seino K, Ishikawa Y, Nozue M, Todoroki T, Fukao K. Impaired proliferative response of Vα24 NKT cells from cancer patients against α-glycosylceramide. J Immunol 2002;168:6494–9.

[18] Taniguchi M, Nakayama T. Recognition and function of Vα14 NKT cells. Immunology 2000;12:543–50.

[19] Deigman T, Curry MP, Doherty DG, et al. Decrease in hepatic CD56+ T cells and Vα24+ natural killer T cells in chronic hepatitis C virus infection. J Hepatol 2002;37:101–8.

[20] Metelitsa LS. Flow cytometry for natural killer T cells: multiparameter methods for multifunctional cells. Clin Immunol 2004;110:267–76.

[21] Picker LJ, Singh MK, Zdraveski Z, et al. Direct demonstration of cytokine synthesis heterogeneity among human memory/effector T-cells by flow cytometry. Blood 1995;86:1408–19.

[22] Godfrey DI, Hammond KJ, Poulton LD, Smyth MJ, Baxter AG. NKT cells: facts, functions and fallacies. Immunol Today 2000;21:573–83.

[23] Valiante NM, D'Andrea A, Crotta S, et al. Life, activation and death of intrahepatic lymphocytes in chronic hepatitis C. Immunol Rev 2000;174:77–89.

[24] Kakimi K, Guidotti LG, Koezuka Y, Chisari FV. Natural killer T cell activation inhibits hepatitis B virus replication in vivo. J Exp Med 2000;192:921–30.

[25] Lucas M, Gadola S, Meier U, et al. Frequency and phenotype of circulating Vα24/Vβ11 double-positive natural killer T cells during hepatitis C virus infection. J Virol 2003;77:2251–7.

[26] Nuti S, Rosa D, Valiante NM, et al. Dynamics of intra-hepatic lymphocytes in chronic hepatitis C: enrichment for Vα24+ T cells and rapid elimination of effector cells by apoptosis. Eur J Immunol 1998;28:3448–55.

[27] Kawarabayashi N, Seki S, Hatsuse K, et al. Decrease of CD56+ T cells and natural killer cells in cirrhotic livers with hepatitis C may be involved in their susceptibility to hepatocellular carcinoma. Hepatology 2000;32:962–9.

[28] Tahir SMA, Cheng O, Shaulov A, et al. Loss of IFN-γ production by invariant NK T cells in advanced cancer. J Immunol 2001;167:4046–50.

Available online at www.sciencedirect.com
SCIENCE DIRECT®
Hepatology Research 34 (2006) 178–186
HEPATOLOGY RESEARCH
http://www.elsevier.com/locate/hepres

The SHAP–hyaluronan complex in serum from patients with chronic liver diseases caused by hepatitis virus infection

Li Shen[a,b], Lisheng Zhuo[a], Akihiko Okumura[c], Tetsuya Ishikawa[c], Masahiko Miyachi[b], Yoshihiro Owa[b], Tohko Ishizawa[d], Nobuo Sugiura[a,d], Yoshihisa Nagata[b], Toshiaki Nonami[b], Shinichi Kakumu[c], Koji Kimata[a,*]

[a] *Institute for Molecular Science of Medicine, Aichi Medical University, Yazako, Nagakute, Aichi 480-1195, Japan*
[b] *Department of Surgery, Aichi Medical University, Yazako, Nagakute, Aichi 480-1195, Japan*
[c] *Department of Internal Medicine, Aichi Medical University, Yazako, Nagakute, Aichi 480-1195, Japan*
[d] *Seikagaku Corporations, Central Research Laboratories, 1253, Tateno 3, Higashiyamato, Tokyo 207-0021, Japan*

Received 14 September 2005; received in revised form 26 December 2005; accepted 27 December 2005
Available online 31 January 2006

Abstract

Our previous study suggested that the serum-derived hyaluronan associated protein (SHAP)–hyaluronan (HA) complex in the sera of patients with rheumatoid arthritis is useful as a marker that directly correlates with the degree of inflammation. Here, we have investigated the serum levels of the SHAP–HA complex in patients at various clinical stages of chronic hepatitis (CH), liver cirrhosis (LC), and hepatocellular carcinoma (HCC) caused by infection with the hepatitis C or hepatitis B virus. Both serum levels of the SHAP–HA complex and HA in those patients were significantly higher than those of the controls and increased in the order of CH < LC < HCC. Different from the HA levels, there was a significant difference in the SHAP–HA complex levels between the LC and HCC groups in both HBV- and HCV-infected patients. In addition, the serum level of the SHAP–HA complex correlated with the well-known biomarkers for liver injury and function such as albumin and platelet, including the HCC indicator alpha-fetoprotein. In conclusion, the present data suggest that the SHAP–HA complex level is a better indicator for the progression of the stages of liver fibrosis, and that it could be a marker for HCC, in both HBV- and HCV-infected patients.

Keywords: Hyaluronan; Chronic hepatitis; Liver cirrhosis; Hepatocellular carcinoma; Inter-α-trypsin inhibitor

1. Introduction

Hyaluronan (HA), a high-molecular weight glycosaminoglycan, is an important component of the mammalian extracellular matrix. HA is synthesized by a variety of cell types, and secreted into the extracellular matrices. Some is released from tissues by degradation, circulated into blood, and is rapidly cleared from the blood by HA receptors-bearing hepatic sinusoidal endothelial cells that take up and degrade HA [1–7]. In recent years, HA has received considerable attention because of various biological functions that have been associated with abnormal cell behaviors and impaired extracellular matrix deposition in liver diseases, including chronic and acute hepatitis [8,9]. A significant increase in serum HA

Abbreviations: SHAP, serum-derived hyaluronan associated protein; HA, hyaluronan; CH, chronic hepatitis; LC, liver cirrhosis; HCC, hepatocellular carcinoma; TSG-6, tumor necrosis factor-stimulated gene-6; HCV, hepatitis C virus; HBV, hepatitis B virus; B-CH, HBV-induced CH; B-LC, HBV-induced LC; B-HCC, HBV-induced HCC; C-LC, HCV-induced LC; C-CH, HCV-induced CH; C-HCC, HCV-induced HCC; ITI, inter-α-trypsin inhibitor; HRP, horseradish peroxidase; BSA, bovine serum albumin; Alb, albumin; ALT, alanine aminotransferase; AFP, α-fetoprotein; Plt, platelet count

* Corresponding author. Tel.: +81 52 264 4811x2088; fax: +81 561 63 3532.
E-mail address: kimata@amugw.aichi-med-u.ac.jp (K. Kimata).

1386-6346/$ – see front matter © 2006 Elsevier Ireland Ltd. All rights reserved.
doi:10.1016/j.hepres.2005.12.008

levels has been reported in patients with chronic liver diseases, especially liver cirrhosis. Serum HA levels may be an index of hepatic fibrosis and sinusoidal endothelial cell function [10–14].

A variety of HA-binding proteins have been reported, such as CD44, versican/PG-M, and TSG-6 (tumor necrosis factor-stimulated gene-6 product) [15–18]. Most of them bind to HA non-covalently, but there is only one exception. Serum-derived hyaluronan-associated protein (SHAP) binds to HA through a covalent bond. SHAP was originally isolated from the extracellular matrix of mouse dermal fibroblasts cultured in the presence of serum [19], and was later identified to be the heavy chains of inter-α-trypsin inhibitor (ITI) family molecules, high-molecular weight glycoproteins synthesized in liver and circulated in blood [20–22]. We previously reported that the serum SHAP–HA levels were significantly increased in patients with rheumatoid arthritis and osteoarthritis and that those levels may be an indicator for inflammation or the reparative processes in the arthritic joints [23]. We found that the SHAP–HA complex is essential for the construction of the cumulus oophorus, where the SHAP–HA complex is one of the major extracellular matrix molecules and the defect of the SHAP–HA complex leads to infertility due to incomplete oocyte maturation and ovulation [24]. Further, we have recently found that the mutant mice hardly suffered from type II collagen-induced arthritis [25], suggesting that the SHAP–HA complex may be an extracellular matrix molecule specifically functioning for inflammatory cells and greatly involved in establishing inflammation, although the mechanism is largely unknown [25,26].

Hepatitis B or C virus (HBV or HCV) infection causes slowly progressive inflammation and is often associated with scarring and architectural changes in liver, which is known as chronic hepatitis (CH). When advanced, it leads to liver cirrhosis (LC). HBV or HCV infection also increases the risk of development of hepatocellular carcinoma (HCC), which is one of the most common human cancers that lead to death [27,28].

In the present study, we measured the serum levels of SHAP–HA complex and HA in patients with chronic hepatitis, liver cirrhosis, and hepatocellular carcinoma with infection of either HCV or HBV, and investigated whether there is any significant relationship between the diagnostic states of each disease and the serum SHAP–HA and HA levels.

2. Materials and methods

2.1. Patients

A total of 396 patients diagnosed with HCV- or HBV-related chronic liver disease (46 patients with B-CH, 100 patients with C-CH, 46 patients with B-LC, 104 patients with C-LC, 33 patients with B-HCC, and 67 patients with C-HCC) were investigated in the present study. All the patients and 27 healthy controls were recruited from Aichi Medical University Hospital, Aichi, Japan. The patients positive for both antibodies to HCV by the third-generation enzyme-linked immunosorbent assay (Lumipulse II, Ortho HCV, Ortho-Clinical Diagnostics, Tokyo, Japan) and HCV-RNA in the sera by RT-PCR assay (AMPLICOR HCV Amplification Kit, Roche Diagnostics, Neuilly, France) were diagnosed as having HCV-related liver disease. The patients positive for both the HBV surface antigen (HBsAg) and HBV DNA in the sera were diagnosed as having HBV-related liver disease. The patients were classified into CH or LC according to the histological findings of their liver biopsy specimens in case liver biopsy was performed within the period of 3 years. About 40% of patients with CH and 10% of patients with LC patients were diagnosed histologically. In case liver biopsy could not be carried out because of some reason such as the risk of bleeding, the patients were classified into these groups according to the levels of platelet counts ($<1 \times 10^5/\mu l$). Diagnosis of HCC was made according to the findings of the CT scan and/or angiography. Blood was drawn from the patients and controls after overnight fasting, and, after separation step, sera was stored in −80 °C until the measurement.

Informed consent was obtained from all patients and healthy controls under the conditions that the project was considered to be reasonable by the Committee at Aichi Medical University in terms of the ethical rules.

2.2. Sandwich ELISA for the measurement of SHAP–HA complex levels in sera

The method has been described previously [23,26]. Reagents used were purchased as follows. Rabbit anti-human ITI antibody was from Dako (Glistrup, Denmark); Maxisorp immunoassay plates, Nunc (Roskilde, Denmark); horseradish peroxidase (HRP)-conjugated goat anti-rabbit IgG antibody, Jackson Immunoresearch Laboratories (West Grove, PA, USA); bovine serum albumin (BSA), Miles Inc. (Kankakee, IL, USA); TMB solution, Moss Inc. (Pasadena, MD); and the HA-binding region of bovine cartilage aggrecan (HABP), Seikagaku Corporation (Tokyo, Japan). A typical standard curve based on the concentrations of the SHAP–HA complex (ng protein/ml) is shown in Fig. 1A. The value for each sample was the mean of triplicate measurements.

2.3. Competitive inhibition ELISA for the measurement of HA levels in sera

Serum HA levels were measured with an IBA kit (Seikagaku Corp., Tokyo, Japan) according to the manufacturer's directions. The principle of this method is as follows: the plates are coated with BSA-conjugated HA, which competes with the soluble HA in the sample solution for the binding of the biotinylated HABP. The amount of biotinylated HABP bound to the immobilized HA was measured by using HRP-conjugated streptavidin and a subsequent color reaction, and was plotted against the HA concentrations in the standard sample solutions to give the standard curve (Fig. 1B), from

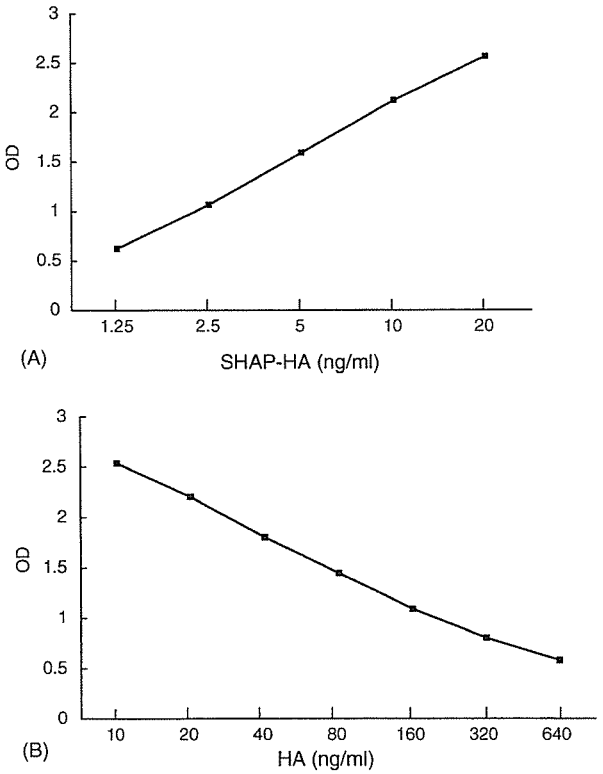

Fig. 1. Representative standard curves of the sandwich ELISA for serum SHAP–HA (A) and competitive inhibition ELISA for serum HA (B). Concentration of SHAP–HA standards (ng/ml) is expressed as the weight content of SHAP protein. Absorbance at 450 nm (OD) at each point is the mean of triplicate measurements, and the deviation of the mean absorbance value for each point was <8%.

which the HA concentrations in the patient samples were calculated. This method detects not only high-molecular weight HA but also low molecular weight HA, in contrast to the sandwich ELISA method that only detects high-molecular weight HA. The value for each sample was the mean of triplicate measurements.

2.4. Serum biochemical markers

The serum levels of albumin (Alb), alanine aminotransferase (ALT), α-fetoprotein (AFP), and platelet (Plt) were measured as diagnostic markers at the Aichi Medical University Hospital. The Alb levels in patient sera are considered to be a marker to evaluate and grade liver function. The ALT levels are known to reflect the degree of liver cell damage. The serum AFP levels are well known to be a major tumor indicator to evaluate HCC. Those marker levels in sera are not available for all the patients whose sera were served for the measurement of SHAP–HA complex and HA levels. Therefore, numbers (n) of the patients for the correlation analysis on the serum levels of SHAP–HA and HA and other biochemical parameters were indicated in the respective tables.

2.5. Statistical analysis

Values were expressed as means ± S.E.M. Statistical analysis of the differences in the serum SHAP–HA and HA levels of HBV- and HCV-infected patients among CH, LC, and HCC was performed by the Steel–Dwass method using Kyplot software, which is the one for multiple comparisons of nonparametric variables. Statistical analysis of the differences in the clinical characteristics of HBV- and HCV-infected patients among CH, LC, and HCC was also performed by the Steel method using Kyplot software. Statistical comparisons of the serum SHAP–HA and HA levels of CH, LC, and HCC between HBV and HCV-infected patients were made using the Mann–Whitney U-test. Correlations of serum levels of SHAP–HA and HA and other biochemical parameters were tested using Pearson's correlation coefficient. Probability values (p) ≤ 0.05 were considered significant.

3. Results

3.1. Clinical characteristics of the patients

Clinical characteristics of the patients were shown in Table 1. Patients at LC stage were older than those at CH stage, and those with HCC were older than those at CH and LC stage, regardless of the etiology of liver disease. Albumin, total cholesterol (T. Chol), and triglycerides (TG), which are considered to be markers to evaluate and grade liver function were decreased in parallel with the progression of the disease. Platelet count (Plt), which is considered to correlate with the degree of liver fibrosis, was also decreased in parallel with the progression of the disease. There was no significant difference in ALT levels between CH, LC, and HCC stages, which are known to reflect the degree of liver cell damage.

3.2. Serum levels of the SHAP–HA complex in patients with chronic liver diseases

We first examined the serum SHAP–HA levels in each group of patients (Fig. 2). The serum SHAP–HA levels in patients with B-CH (29 ± 18 ng/ml), B-LC (60 ± 56 ng/ml), and B-HCC (101 ± 77 ng/ml) were significantly higher than those of the controls (14.1 ± 2.7 ng/ml) ($p < 0.01$ in all cases). The SHAP–HA levels in the B-LC group were significantly higher than those in the B-CH group ($p < 0.01$), and those in B-HCC were further significantly higher than those in the B-LC group ($p < 0.01$). The serum SHAP–HA levels in patients with C-CH (36 ± 25 ng/ml), C-LC (62 ± 48 ng/ml), and C-HCC (110 ± 89 ng/ml) were also significantly higher than those of controls ($p < 0.01$ in all cases). The SHAP–HA levels in the C-LC group were significantly increased when compared with those in the C-CH group ($p < 0.01$). Similarly, the patients with C-HCC showed further higher SHAP–HA levels than those with C-LC ($p < 0.01$). A comparison among the SHAP–HA levels in those patients indicated that the lev-

Table 1
Clinical characteristics of the patients with chronic liver disease

	HBV-related			HCV-related		
	CH	LC	HCC	CH	LC	HCC
M : F	31 : 15	35 : 11	20 : 13	58 : 42	52 : 52	42 : 25
Age (years)	42±13	55±10	59±7	56±11	62±12	68±7
ALT (IU/ml)	55±50	38±26	53±49	68±78	67±40	63±32
Albumin (mg/dl)	4.3±0.5	4.2±0.5	3.9±0.7	4.4±0.3	4.0±0.5	3.7±0.5
T. Chol (mg/dl)	184±25	190±33	143±34	181±33	136±42	142±37
TG (mg/dl)	108±74	100±39	85±39	127±53	99±36	101±49
Hb (g/dl)	14.0±1.4	14.4±0.3	13.1±1.5	14.1±1.5	13.3±2.1	12.4±1.8
Plt (x10^4/μl)	16.2±5.5	12.4±4.1	9.0±3.7	18.6±5.7	10.4±4.1	9.5±4.3

ALT, alanine aminotransferase; T. Chol, total cholesterol; TG, triglycerides; Hb, hemoglobin; Plt, platelets.
$^{*}p<0.05$, $^{**}p<0.01$.

els of SHAP–HA in the HCV-groups had a tendency to be higher than those in the HBV groups, especially at the CH stage ($p=0.05$).

Sera of patients infected with HCV or HBV have tendency that albumin, cholesterol, platelets, etc. were lowered (see Table 1). Because the patients with HCC would have problem with the lowering liver functions (see the details in the latter Section 3.5). Therefore, the increased levels of the SHAP–HA complex in sera of those patients would not simply reflect the carcinogenesis. To clarify those points, we examined and compared the serum levels of the SHAP–HA complex between the patients with HCC ($n=31$) and those with LC ($n=30$) whose albumin concentrations in sera were both higher than 4.0 g/dl. The levels showed 75.6 ± 60.4 and 47.9 ± 32.6 ng/ml, respectively, and were significantly high in sera of the HCC, compared with those of the LC ($p=0.03$). Similarly, the patients with HCC ($n=38$) and those with LC ($n=19$) whose platelet numbers in blood were at the same range (5–12 × 10^4/μl) showed the SHAP–HA complex levels of 97.8 ± 71.3 and 61.5 ± 32.4 ng/ml, respectively ($p=0.04$). Even when some of the serum conditions were similar to each other, the SHAP–HA complex levels in sera of HCC were still higher than those in sera of LC. It is very likely, therefore, that the increased levels of the SHAP–HA complex in sera could reflect the carcinogenesis.

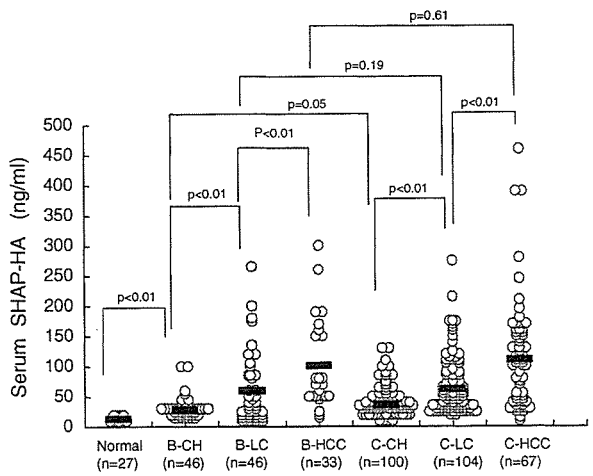

Fig. 2. Serum levels of the SHAP–HA complex in patients with B-CH, B-LC, B-HCC, C-HC, C-LC and C-HCC, and in healthy controls. The concentrations are measured by sandwich ELISA. The horizontal bars denote the mean value in each group. Standard deviations of these mean values are described in the text. The p-values between the HBV- and HCV-groups were obtained by the Mann–Whitney's test, and those among HC, LC, and HCC groups were obtained by the Steel–Dwass method using Kyplot software for multiple comparisons.

3.3. Serum levels of HA in patients with chronic liver diseases

We then examined the serum HA levels in each group of patients (Fig. 3). The serum HA levels were 228 ± 229 ng/ml in the B-CH group, 841 ± 811 ng/ml in the B-LC group, and 1170 ± 1436 ng/ml in the B-HCC group, all being significantly higher than those of the controls (52.4 ± 10.5 ng/ml) ($p<0.01$ in all cases). The serum HA levels in the patients with C-CH (403 ± 485 ng/ml), C-LC (1280 ± 1421 ng/ml), and C-HCC (1374 ± 1 364 ng/ml) were also significantly higher than those of the controls ($p<0.01$ in all cases). In both the HBV- and HCV-groups, the HA levels in the LC patients were significantly higher than those in the CH group (both $p<0.01$). However, in contrast to the SHAP–HA levels,

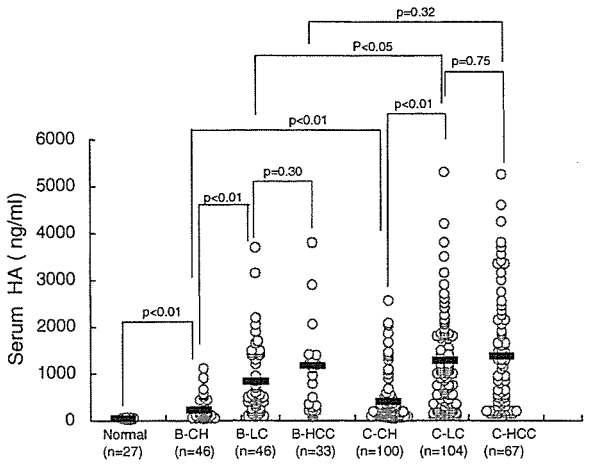

Fig. 3. Serum levels of HA in patients with B-CH, B-LC, B-HCC, C-HC, C-LC and C-HCC, and in healthy controls. The concentrations were measured with competitive inhibition ELISA. The horizontal bars denote the mean value in each group. Standard deviations of these mean values are described in the text. The p-values between the HBV- and HCV-groups were obtained by the Mann–Whitney's test, and those among HC, LC, and HCC groups were obtained by the Steel–Dwass method using Kyplot software for multiple comparisons.

there was no further significant increase of serum HA levels in the HCC groups ($p=0.30$ and 0.75 in HBV- and HCV-groups, respectively). When a comparison between the HBV- and HCV-groups was made, HCV-infected patients showed significantly higher serum HA levels at the CH and LC stages (C-CH versus B-CH, $p<0.01$; C-LC versus B-LC, $p<0.05$), but not at the HCC stage (C-HCC versus B-HCC, $p=0.32$).

3.4. Positive correlations between serum levels of SHAP–HA complex and HA in chronic liver diseases

We further investigated whether there are any correlations between the serum levels of the SHAP–HA complex and HA at each stage of chronic liver disease (Table 2). Significant positive correlations were found between the levels of the SHAP–HA complex and HA at all stages in both HBV- and HCV-groups. The r-value was highest in C-HCC ($r=0.84$) and was lowest in C-CH ($r=0.41$). Thus the r-value varied according to the status of the liver disease, suggesting the difference in the mechanisms in the formation of SHAP–HA complex. No significant correlation was found in the healthy control groups.

Table 2
Correlation between serum levels of SHAP–HA complex and HA

Samples	n	r	p-Value
Control	27	0.20	NS
B-CH	46	0.67	<0.0001
B-LC	46	0.73	<0.0001
B-HCC	33	0.67	<0.0001
C-CH	100	0.41	<0.0001
C-LC	104	0.70	<0.0001
C-HCC	67	0.84	<0.0001

The null hyaluronan, $r=0$, against the alternative $r\neq 0$. NS: not significant.

The serum levels of the SHAP–HA complex and HA at each stage of chronic liver disease were also comparatively investigated. Averaged ratios of the SHAP–HA complex to HA was 0.095 ± 0.094 and 0.186 ± 0.273 for C-LC and for C-HCC, respectively, and 0.103 ± 0.075 and 0.184 ± 0.194 for B-LC and for B-HCC, respectively, although statistical significant values given by the Mann–Whitney U-test were $p<0.05$ and $p=0.135$ for the former and latter comparisons, respectively, and the latter high value (i.e. low significance) was probably due to the less sample number ($n=33$). Thus, it is possible to consider ratios of the SHAP–HA to HA levels as well as their respective levels as diagnostic and prognostic indexes to monitor trends of changes in the disease state from LC to HCC.

3.5. Correlations of the serum SHAP–HA and HA levels with other biochemical parameters in patients with chronic liver diseases

The correlations of serum levels of the SHAP–HA complex and HA in each disease stage with other biochemical parameters were investigated (Tables 3 and 4). In HBV-related chronic liver diseases, significant correlations were found between the serum levels of HA, Alb, and Plt, at the CH stage. This was also the case for the serum levels of the SHAP–HA complex. At the LC stage, only the serum levels of SHAP–HA complex but not HA correlated with the levels of Alb and Plt. At the HCC stage, there was neither correlation between the serum levels of the HA and these parameters, nor

Table 3
Correlation between serum levels of HA/SHAP–HA complex and clinical variables in patients with HBV-related chronic liver diseases

	CH ($n=46$)				LC ($n=46$)				HCC ($n=33$)			
	HA		SHAP–HA		HA		SHAP–HA		HA		SHAP–HA	
	r^*	p^{**}	r	p	r	p	r	p	r	p	r	p
Alb	−0.56	<0.01	−0.60	<0.01	−0.40	NS	−0.57	<0.01	−0.29	NS	−0.49	NS
ALT	0.29	NS	0.22	NS	0.35	NS	0.20	NS	0.06	NS	−0.16	NS
Plt	−0.55	<0.05	−0.58	<0.05	−0.37	NS	−0.64	<0.05	0.22	NS	0.21	NS

* r-Value.
** p-Value.

Table 4
Correlation between serum levels of HA/SHAP–HA complex and clinical variables in patients with HCV-related chronic liver diseases

	CH ($n=100$)				LC ($n=104$)				HCC ($n=67$)			
	HA		SHAP–HA		HA		SHAP–HA		HA		SHAP–HA	
	r^*	p^{**}	r	p	r	p	r	p	r	p	r	p
Alb	−0.37	<0.01	−0.39	<0.01	−0.09	NS	−0.44	<0.05	−0.21	NS	−0.37	<0.01
ALT	0.02	NS	0.08	NS	0.04	NS	0.04	NS	0.32	<0.05	0.33	<0.05
Plt	−0.05	NS	−0.44	<0.01	−0.18	NS	−0.45	<0.05	−0.17	NS	−0.24	NS

* r-Value.
** p-Value.

Table 5
Correlation of serum levels of SHAP–HA and HA with levels of AFP in patients bearing HCC

	HA		SHAP–HA	
	r-Value	p-Value	r-Value	p-Value
B-HCC ($n=33$)	−0.02	NS	0.63	<0.05
C-HCC ($n=67$)	0.07	NS	0.31	<0.05

between the serum SHAP–HA levels and these parameters. On the other hand, in HCV-related chronic liver diseases, the serum levels of the SHAP–HA complex correlated significantly with the levels of Alb and Plt at the CH stage, while serum HA levels correlated only with serum levels of Alb. At the LC stage, serum levels of the SHAP–HA complex still had a significant correlation with the levels of Alb and Plt. At the HCC stage, serum levels of both HA and SHAP–HA complex correlated with that of ALT, and the serum SHAP–HA levels still had a significant correlation with the levels of Alb.

3.6. Correlations of the serum SHAP–HA and HA levels with AFP levels in patients bearing HCC

Since the patients with HCC showed further higher serum SHAP–HA levels than those with LC regardless of the difference of viruses infected, we investigated whether the serum levels of SHAP–HA complex correlate with AFP, one of the well-known marker for HCC. Serum levels of SHAP–HA complex had a significant correlation with AFP levels, but those of HA did not (Table 5).

4. Discussion

The SHAP–HA complex is the modified form of the HA molecule. In contrast to the daily turnover of considerable amounts of HA, the SHAP–HA complex apparently occurs only under unusual circumstances, especially during inflammatory responses. It is already known that this situation occurs in the inflamed synovia of rheumatoid arthritis patients [23,26]. We have shown that the formation of the SHAP–HA complex requires, in addition to HA and ITI family molecules as substrates, enzyme factor(s) that are also present in plasma [19,24]. The enzyme factors catalyze the transfer of the heavy chains from the chondroitin sulfate chain of the bikunin portion to HA, accompanied by the release of bikunin [24,25].

Considering the above characteristics of the SHAP–HA complex formation, the following circumstances could give rise to the high levels of the complex in sera from patients with the liver diseases. An abnormally high amount of HA is synthesized and accumulates in tissues of the diseased liver such as LC and HCC [29,30], and there are the abnormal development and organization of blood circulation systems [31]. Such conditions make it possible to supply the ITI family molecules and enzyme factor(s) directly to the tissue HA. Consequently, the abnormal formation and accumulation of the SHAP–HA complex likely occur within the diseased liver and some of the complex leaks into the blood circulation. Under normal conditions, HA is released from tissues into the circulation and cleared in the liver. Although the HA encounters the ITI family molecules and enzyme factor(s) in the circulation, the formation reaction proceeds slowly [20,24] and the clearance rate of the HA is too fast to receive the modification to form the SHAP–HA complex [4]. However, when the liver function is impaired in the diseased liver, the degradation of HA slows down, which results in the accumulation of HA. Consequently, the HA has more chance of undergoing the modification.

Marked increases of serum HA levels in chronic liver disease have been reported before [8,12–14,32–39]. Several studies have evaluated the measurement of the serum HA level as a useful indicator for assessing the severity of liver injury and fibrosis [3,12,32–34]. McHutchison et al. [12] reported not only significant elevation of the serum HA levels in patients with C-CH but also a correlation with the degree of fibrosis in the liver. Pontinha et al. [8] confirmed that the serum HA levels in patients with B-CH are useful for assessing and monitoring time trends in the disease state. Das et al. [31] reported that the serum HA levels are useful to estimate the functional hepatic reserve as preoperative risk factors in patients with LC. Frebourg et al. [34] suggested that the increase of serum HA levels in chronic liver disease is due to the excessive production of HA, while Engstrom et al. [35] claimed that liver fibrosis changes the tissue structures which cause a reduction in the HA uptake and degradation activity in hepatic sinusoidal endothelial cells. Although it is still under question as to which possibility is more likely,

increased levels of HA in the sera have an effect on the serum levels of the SHAP–HA complex.

The major aim of this study is to examine the change of serum levels of the SHAP–HA complex and, if any, the correlations with those of HA along with the progression of hepatitis virus infection-induced chronic liver diseases (from CH to LC, then to HCC), and explore its potential to serve as a marker for assessing the severity of liver injury and fibrosis.

Our present results of the serum HA levels confirmed the significant elevation in the patients with virus-induced chronic liver diseases (Fig. 3). As expected, elevation was also found in the serum levels of the SHAP–HA complex (Fig. 2), and it showed significant but different correlation with the HA levels at each stage of chronic liver disease (Table 2), which supports our hypothesis that the complex formation depends on the availability of HA and also suggests that the serum SHAP–HA levels are more preferential as a marker for the diagnosis of chronic liver disease as discussed below.

In both HBV- and HCV-infected patients, a significant elevation of serum HA levels was found compared with the healthy controls and CH group, more strikingly between the CH and LC groups, but not between the LC and HCC groups, indicating that the serum HA level reflects the inflammatory and cirrhotic processes, but not the tumorigenic process (Fig. 3). In contrast, there is a significant elevation of the serum levels of the SHAP–HA complex between the LC and HCC groups (Fig. 2). The finding suggests that the SHAP–HA complex levels relate more closely than the HA levels to the tumorigenic progress. This is also confirmed in Table 5 to show significant correlation of the serum AFP levels with the serum SHAP–HA levels but not with the serum HA levels. Recent reports have shown that the serum level of PIVKA-II (protein induced by Vitamin K absence or antagonists II)/DCP (des-γ-carboxy prothrombin) is the more useful predisposing clinical parameter than that of AFP for the development of portal venous invasion in patients with HCC [40,41]. Therefore, it should be worthy examining the correlation between DCP and the SHAP–HA complex levels in sera of those patients. In relation to the increase of the SHAP–HA complex levels, TSG-6 has recently been observed to enhance the formation reaction or be itself involved in the reaction as an enzyme [42,43]. We previously observed that PG-M/versican enhanced the formation reaction in vitro by binding to both ITI and HA to form a tertiary complex where the transesterification reaction may be accelerated [44,45]. PG-M/versican is often found as a component of the tumorigenic extracellular matrix [46]. Therefore, those factors may contribute to the increase in the efficiency of the formation of the complex and result in a higher ratio of the SHAP–HA complex to HA as seen in the case of HCC. Thus, it is possible to consider ratios of the SHAP–HA to HA levels as well as their respective levels as diagnostic and prognostic indexes to monitor trends of changes in the disease state from LC to HCC.

We then investigated the correlation of the serum levels of the SHAP–HA complex and HA with other biomarkers which represent liver functions and injury. Both the levels negatively correlate with Alb and Plt in the most serum samples, indicating that the serum levels of the SHAP–HA complex and HA do reflect the decreased liver function and degree of liver fibrosis. It is of note that a better correlation with these biomarkers was frequently found in the serum levels of the SHAP–HA complex than in the HA levels, particularly in LC stage. Interestingly, no significant correlation was found between these biomarkers and serum levels of SHAP–HA complex in B-HCC group, whereas both the serum levels of HA and SHAP–HA had a weak correlation with ALT levels in C-HCC. A different panel of correlations with the biomarkers observed between the HBV- and HCV-infected patients may be explained at the present time by possible differences in the mechanisms and processes for the infection and the induction of liver diseases between hepatitis C and B viruses.

Although we have shown the positive correlation between the SHAP–HA complex level and the hepatocellular carcinogenesis, sera of patients infected with HCV or HBV have significant tendency that albumin, cholesterol, platelets, etc. were lowered as shown in Table 1. Those would have been caused by the lowering liver functions and the decrease of the platelets of the patients with HCC. Therefore, the increased levels of the SHAP–HA complex in sera of those patients might not simply reflect the carcinogenesis. However, even if we compared the serum levels of the SHAP–HA complex between the patients with HCC and those with LC whose albumin concentrations in sera were above 4.0 g/dl and also whose platelet numbers in blood were almost at the same range, the SHAP–HA complex levels in sera of HCC were still higher than those in sera of LC. Thus, we could consider that the increased levels of the SHAP–HA complex in sera could reflect the carcinogenesis. If we had the patients with the progression from LC to HCC, it should be worthy to follow-up the changes of the SHAP–HA complex levels during the processes.

Considering those results together, the serum levels of the SHAP–HA complex may be a useful index not only for monitoring functional changes of the liver in patients with chronic hepatitis and liver cirrhosis, but also for the diagnosis of progression to hepatocellular carcinoma, where it is superior to using the serum level of HA.

Acknowledgements

We are grateful to Drs. M. Yoneda and T. Yada for their helpful discussion. This work was supported by a Grant-in-Aid for Scientific Research (B) from the Japan Society for the Promotion of Science (JSPS); in part, by a Grant-in-Aid for Scientific Research on Priority Areas (14082206) from the Ministry of Education, Culture, Sports, Science and Technology of Japan; and by a special research fund from the Seikagaku Corporation.

References

[1] McGary CT, Raja RH, Weigel PH. Endocytosis of hyaluronic acid by rat liver endothelial cell. Evidence for receptor recycling. Biochem J 1989;257:875–84.

[2] Lebel L, Fraser JR, Kimpton WS, Gabrielsson J, Gerdin B, Laurent TC. A pharmacokinetic model of intravenously administered hyaluronate in sheep. Pharm Res 1989;6:677–82.

[3] Laurent TC, Fraser JR. The properties and turnover of hyaluronan. In: Functions of protoglycans, Ciba Foundation Symposium 124. Chichester: Wiley; 1986. p. 9–29.

[4] Laurent TC, Fraser JR. Hyaluronan. FASEB J 1992;6:2397–404.

[5] Laurent TC, Laurent UB, Fraser JR. The structure and function of hyaluronan: an overview. Immunol Cell Biol 1996;74:A1–7.

[6] Fraser JR, Laurent TC. Hyaluronan. In: Comper WD, editor. Extracellular matrix, vol. 2. Amsterdam: Harwood Academic Publishers; 1996. p. 141–99.

[7] Eriksson S, Fraser JR, Laurent TC, Pertoft H, Smedsrod B. Endothelial cell are a sit of uptake and degradation of hyaluronic acid in the liver. Exp Cell Res 1983;144:223–8.

[8] Pontinha N, Pessegueiro H, Barros H. Serum hyaluronan as a marker of liver fibrosis in asymptomatic chronic virus hepatitis B. Scand J Clin Lab Invest 1999;59(5):343–7.

[9] Suzuki K, Endo R, Takikawa Y, Nakadate I, Sato S. Serum hyaluronate in patients with acute and fulminant hepatitis. J Gastroenterol 1996;31:237–41.

[10] Ogata T, Okuda K, Ueno T, Saito N, Aoyagi S. Serum hyaluronan as a predictor of hepatic regeneration after hepatectomy in humans. Eur J Clin Investig 1999;29:780–5.

[11] Satoh T, Ichida T, Matsuda Y, et al. Interaction between hyaluronan and CD44 in the development of dimethylnitrosamine-induced liver cirrhosis. J Gastroen Hepatol 2000;15:402–11.

[12] McHutchison JG, Blatt LM, de Medina M, et al. Measurement of serum hyaluronic acid in patients with chronic hepatitis C and its relationship to liver histology. J Gastroen Hepatol 2000;15:945–51.

[13] Grzeszczuk A, Lapinski TW, Panasiuk A. Levels of hyaluronic acid in chronic virus C hepatitis with relationship to liver steatosis. Wiad Lek 2002;55(1–2):35–41.

[14] Kopke-Aguiar LA, Martins JR, Passerotti CC, Toledo CF, Nader HB, Broges DR. Serum hyaluronic acid as a comprehensive marker to assess severity of liver disease in schistosomiasis. Acta Trop 2002;84(2):117–26.

[15] Toole BP. Hyaluronan and its binding proteins, the hyaladherins. Curr Opin Cell Biol 1990;2:839–44.

[16] Fosang JA, Hardingham TE. Matrix proteoglycans. In: Comper WD, editor. Extracellular matrix, vol. 2. Amsterdam: Harwood Academic Publishers; 1996. p. 200–29.

[17] Lee TH, Wisniewski HG, Vilcek J. A novel secretory tumor necrosis factor-inducible protein (TSG-6) is a member of the family of hyaluronate binding proteins, closely related to the adhesion receptor CD44. J Cell Biol 1992;116:5455–7.

[18] Shinomura T, Nishida Y, Ito K, Kimata K. cDNA cloning of PG-M, a large chondroitin sulfate proteoglycan expressed during chondrogenesis in chick limb buds. Alternative spliced multiforms of PG-M and their relationship to versican. J Biol Chem 1993;268:14461–9.

[19] Yoneda M, Suzuki S, Kimata K. Hyaluronic acid associated with the surfaces of cultured fibroblasts is linked to a serum-derived 85 kDa protein. J Biol Chem 1990;265:5247–57.

[20] Huang L, Yoneda M, Kimata K. A serum-derived hyaluronan-associated protein (SHAP) is the heavy chain of the inter-α-trypsin inhibitor. J Biol Chem 1993;268:26725–30.

[21] Zhao M, Yoneda M, Ohashi Y, et al. Evidence for the covalent binding of SHAP, heavy chain of inter-α-trypsin inhibitor, to hyaluronan. J Biol Chem 1995;270:26657–63.

[22] Enghild JJ, Salvesen G, Hefta SA, Thogersen IB, Rutherfurd S, Pizzo SV. Chondroitin 4-sulfate covalently cross-links the chains of the human blood protein pre-alpha-inhibitor. J Biol Chem 1991;266:747–51.

[23] Kida D, Yoneda M, Miyaura S, et al. The SHAP–HA complex in sera from patients with rheumatoid arthritis and osteoarthritis. J Rheumatol 1999;26:1230–8.

[24] Zhuo L, Yoneda M, Zhao M, et al. Defect in SHAP-hyaluronan complex causes severe female infertility. J Biol Chem 2001;276:7693–6.

[25] Zhuo L, Shen L, Nonogaki T, et al. Biological function of hyaluronan-SHAP covalent complex. In: Garg HG, Hales CA, editors. Chemistry and biology of hyaluronan. Amsterdam: Elsevier; 2004. p. 205–22.

[26] Yingsung W, Zhuo L, Morgelin M, et al. Molecular heterogeneity of the SHAP–hyaluronan complex: isolation and characterization of the complex in synovial fluid from patients with rheumatoid arthritis. J Biol Chem 2003;278:32710–8.

[27] Fattovich G, Giustina G, Degos F, et al. Morbidity and mortality in compensated cirrhosis type C: a retrospective follow-up study of 384 patients. Gastroenterology 1997;112:463–72.

[28] Tong MJ, Lee SY, Hwang SJ, et al. Evidence for hepatitis C virus infection in patients with primary hepatocellular carcinoma. West J Med 1994;160:133–8.

[29] Murata K, Ochiai Y, Akashio K. Polydispersity of acidic glycosaminoglycan components in human liver and the changes at different stages in liver cirrhosis. Gastroenterology 1985;89:1248–57.

[30] Gressner AM, Haarmann R. Regulation of hyaluronate synthesis in rat liver fat storing cell cultures by Kupffer cells. J Hepatol 1988;7:310–8.

[31] Ueno T, Sata M, Tanikawa K. Cells responsible for extracellular matrix production in the liver. In: Okazaki I, Ninomiya Y, Friedman SL, Tanikawa K, editors. Extracellular matrix and the liver: approach to gene therapy. Amsterdam: Academic Press; 2003. p. 89–103.

[32] Gibson PR, Fraser JR, Brown TJ, et al. Hemodynamic and liver function predictors of serum hyaluronan in alcoholic liver disease. Hepatology 1992;15:1054–9.

[33] Grzeszczuk A, Chlabicz S, Panasiuk A. Serum hyaluronan as a possible biomarker of liver insufficiency cirrhosis patients. Rocz Akad Med Bialymst 2002;47:80–5.

[34] Das BC, Isaji S, Kawarada Y. Analysis of 100 consecutive hepatectomies: risk factors in patients with liver cirrhosis or obstructive jaundice. World J Surg 2001;25:266–73.

[35] Frebourg T, Delpech B, Bercoff E, et al. Serum hyaluronate in liver diseases: study by enzymoimmunological assay. Hepatology 1986;6:392–5.

[36] Engstrom-Laurent A, Loof L, Nyberg A, Schroder T. Increased serum hyaluronate in liver disease. Hepatology 1985;5:638–42.

[37] Hasegawa T, Sasaki T, Kimura T, et al. Measurement of serum hyaluronic acid as a sensitive marker of liver fibrosis in biliary atresia. J Pediatr Surg 2000;35(11):1643–6.

[38] Wyatt HA, Dhawan A, Cheeseman P, Mieli-Vergani G, Price JF. Serum hyaluronic acid concentrations are increased in cystic fibrosis patients with liver disease. Arch Dis Child 2002;86:190–3.

[39] Yachida S, Wakabayashi H, Kokudo Y, et al. Measurement of serum hyaluronate acid as a predictor of human liver failure after major hepatectomy. World J Surg 2000;24:359–64.

[40] Suehiro t, Sugimachi K, Matsumura T, Itasaka H, Taketomi A, Maeda T. Protein induced by Vitamin K absence or antagonist II as a prognostic marker in hepatocellular carcinoma. Cancer 1994;73:2464–71.

[41] Koike Y, Shiratori Y, Sato S, et al. Des-γ-carboxy prothrombin as a useful predisposing factor for the development of portal venous invasion in patients with hepatocellular carcinoma. Cancer 2001;91:561–9.

[42] Jessen TE, Odum L. Role of tumour necrosis factor stimulated gene 6 (TSG-6) in the coupling of inter-a-trypsin inhibitor to hyaluronan in human follicular fluid. Reproduction 2003;125:27–31.

[43] Fulop C, Szanto S, Mukhopadhyay D, et al. Impaired cumulus mucification and female sterility in tumor necrosis factor-induced protein-6 deficient mice. Development 2003;130:2253–61.
[44] Yoneda M, Zhao M, Zhuo L, et al. Role of inter-α-trypsin Inhibitor and hyaluronan-binding proteoglycans in hyaluronan-rich matrix formation. In: Abatangelo G, Weigel PH, editors. Redefining hyaluronan. Amsterdam: Elsevier; 2000. p. 21–30.
[45] Zhao M, Yoneda M, Zhuo L, et al. In: Kennedy JF, Phillips GO, Williams PA, Hascall VC, editors. Hyaluronan: chemical, biochemical and biological aspects. Cambridge: Woodhead Publishing Ltd.; 2002. p. 497–500.
[46] Nakashima N, Sobue M, Fukata S, et al. Immunohistochemical characterization of extracellular matrix components of yolk sac tumors. Virchows Arch B Cell Pathol Incl Mol Pathol 1990;58(4):309–15.